Recent Advances in Stability and Failure Mechanisms of Landslide Dams

frontiers in Earth Science

REVIEW
published: 29 March 2021
doi: 10.3389/feart.2021.659935

Recent Advances in Stability and Failure Mechanisms of Landslide Dams

Hongchao Zheng[1,2], Zhenming Shi[1,2], Danyi Shen[1,2], Ming Peng[1,2], Kevin J. Hanley[3], Chenyi Ma[1,2] and Limin Zhang[4]*

[1] Key Laboratory of Geotechnical and Underground Engineering of Ministry of Education, Department of Geotechnical Engineering, Tongji University, Shanghai, China, [2] Department of Geotechnical Engineering, College of Civil Engineering, Tongji University, Shanghai, China, [3] School of Engineering, Institute for Infrastructure and Environment, The University of Edinburgh, Edinburgh, United Kingdom, [4] Department of Civil and Environmental Engineering, Hong Kong University of Science and Technology, Hong Kong, Hong Kong

Numerous landslide dams have been induced in recent years as a result of frequent earthquakes and extreme climate hazards. Landslide dams present serious threats to lives and properties downstream due to potentially breaching floods from the impounded lakes. To investigate the factors influencing the stability of landslide dams, a large database has been established based on an in-depth investigation of 1,737 landslide dam cases. The effects of triggers, dam materials, and geomorphic characteristics of landslide dams on dam stability are comprehensively analyzed. Various evaluation indexes of landslide dam stability are assessed based on this database, and stability evaluation can be further improved by considering the dam materials. Stability analyses of aftershocks, surges, and artificial engineering measures on landslide dams are summarized. Overtopping and seepage failures are the most common failure modes of landslide dams. The failure processes and mechanisms of landslide dams caused by overtopping and seepage are reviewed from the perspective of model experiments and numerical analyses. Finally, the research gaps are highlighted, and pathways to achieve a more complete understanding of landslide dam stability are suggested. This comprehensive review of the recent advances in stability and failure mechanisms of landslide dams can serve as a key reference for stability prediction and emergency risk mitigation.

Keywords: landslide dam stability, influencing factor, overtopping failure, seepage failure, aftershock, surge

OPEN ACCESS

Edited by:
Tao Zhao,
Brunel University London,
United Kingdom

Reviewed by:
Tingkai Nian,
Dalian University of Technology, China
Chong Xu,
National Institute of Natural Hazards,
Ministry of Emergency Management (China), China

***Correspondence:**
Ming Peng
pengming@tongji.edu.cn

Specialty section:
This article was submitted to Geohazards and Georisks, a section of the journal Frontiers in Earth Science

Received: *28 January 2021*
Accepted: *04 March 2021*
Published: *29 March 2021*

Citation:
Zheng H, Shi Z, Shen D, Peng M, Hanley KJ, Ma C and Zhang L (2021) Recent Advances in Stability and Failure Mechanisms of Landslide Dams. Front. Earth Sci. 9:659935. doi: 10.3389/feart.2021.659935

INTRODUCTION

Landslide dams are natural dams formed by river blockages with massive amounts of materials from avalanches, landslides, or debris flows (Swanson et al., 1986; Capra, 2006; Korup and Tweed, 2007; Hermanns, 2013; Shi et al., 2014). A large number of landslide dams have been induced by frequent earthquakes (Huang and Fan, 2013; Fan et al., 2014), extreme climate hazards (Dong et al., 2011; Gariano and Guzzetti, 2016), or snowmelt (Costa and Schuster, 1991; Strom, 2010; Frey et al., 2018). For instance, multiple landslide dams were clustered along short river reaches induced by the 1999 Chi-Chi earthquake (Liao and Lee, 2000), the 2004 Chuetsu earthquake (Wang et al., 2007), and the

2008 Wenchuan earthquake (Fan et al., 2012). Eighteen landslide dams were formed by the 2009 Morakot typhoon in Taiwan (Chen and Chang, 2016). Landslide dams have frequently occurred in the rivers on the Tibetan Plateau, caused by slides and debris flows induced by snowmelt water or active glaciers (Fan et al., 2019; Wang et al., 2020).

Landslide dams present serious threats to lives and properties downstream from a potentially rapid release of the impounded water if the dams fail (Huang and Fan, 2013; Fan et al., 2014). This threat is greater for some landslide dams with large volumes: if loss of stability occurs, the breached floods could be hundreds of times the maximal recorded floods in history, and could destroy almost everything in their paths (Schuster, 2000; Hegan et al., 2001; Yin et al., 2009). The evaluation of landslide dam stability is thus crucial before taking any effective mitigation measures.

The stability of a landslide dam is usually difficult to determine. The formation and instability of landslide dams are regulated by the complex interactions between the geomorphological parameters of the valley (geometries of landslide dam and lake), the slide characteristics (dam material), and the hydrological parameters of the river (inflow rate and lake volume). Moreover, landslide dam stability is affected by aftershocks, surge actions, and human control measures.

Korup (2002) reviews the geomorphic assessment indexes of landslide dam stability and points out that there is still a considerable lack of understanding regarding the stability and failure mechanisms of landslide dams. Since then, landslide dam cases on a regional and global scale have been widely collected to obtain their spatial morphology and distribution regularity (Fan et al., 2020). Based on these field cases, the effects of the characteristic parameters on landslide dam stability have been explored (Ermini and Casagli, 2003; Evans et al., 2011). In addition, evaluation models of landslide dam stability have been established by means of statistical analysis (Dong et al., 2009; Shen et al., 2020). Subsequently, the failure mechanisms of landslide dams caused by overtopping and seepage have been explored using model experiments and numerical analyses (Shi et al., 2015a,b,c; Zhou G.G.D. et al., 2019; Zhou M. et al., 2019). However, there are few comprehensive reviews of the stability and failure mechanisms of landslide dams.

In this study, a large database with 1,737 landslide dam cases worldwide is compiled to give a comprehensive perspective of landslide dam stability. Based on this database, the effects of the characteristic parameters on landslide dam stability are first reviewed in Section "Influences of Characteristic Parameters on Landslide Dam Stability." Stability analyses of aftershocks, surges, and artificial engineering measures on the landslide dams are summarized in Section "Stability Analyses of Special Factors on Landslide Dams." Then, detailed investigations of failure mechanisms of landslide dams caused by overtopping and seepage are reviewed in Sections "Overtopping Failure Analyses of Landslide Dams" and "Seepage Failure Analyses of Landslide Dams," respectively. Finally, research gaps and pathways are highlighted in Section "Future Research Directions." An exhaustive review of the recent advances in stability and failure mechanisms of landslide dams can provide a reliable basis for stability prediction, early warning, and emergency risk mitigation in mountainous areas.

INFLUENCES OF CHARACTERISTIC PARAMETERS ON LANDSLIDE DAM STABILITY

In this section, the effects of single and multiple characteristic parameters on landslide dam stability are reviewed. A database containing 1,737 landslide dams located in 45 countries and regions has been assembled over a decade through literature review (Shen et al., 2020), to provide detailed insight into the stability of landslide dams.

The distribution of landslide dams is closely related to seismic zones worldwide as shown in **Figure 1**. Landslide dams are widely distributed in China, Italy, Japan, and the United States, due to a wide range of mountainous regions and numerous seismic belts. By contrast, few landslide dams documented in the literature occur in Africa.

Due to uncertainties in the life periods and failure modes of landslide dams, their stability can be difficult to determine. A landslide dam might have existed for several decades or even hundreds of years, but its ultimate failure may be caused by a heavy rainstorm or other factors. In this paper, a landslide dam is called stable when a backwater lake still exists or is filled in with sediments at the time of its analysis (Fan et al., 2020). Those classified as "unstable" have encountered a catastrophic breach with the abrupt release of the impounded lake waters or piping having developed from upstream to downstream of the dam.

Landslide dam failure could be induced by overtopping, piping or downstream slope slide (Shi et al., 2018; Fan et al., 2020). Overtopping failures appear where landslide dams undergo erosion or collapse leading to a catastrophic breach, with the subsequent release of the impounded lake waters (**Figures 2A–C**). Piping gradually develops when small particles are transported to free exits or into coarse openings driven by hydraulic gradient and lake waters are released through the leakage channel (**Figure 2D**). Downstream slope failures occur where the buoyant weight of the downstream dam is lower than the uplift force with a rapid increase in the upstream water level.

Overtopping failure is the most common instability mode, accounting for approximately 90% of the inventoried landslide dams which fail (**Figure 3**), whereas seepage failure is less common. The failure situation is significantly different from that of embankment dams (Foster et al., 2000; Richards and Reddy, 2007). The width of landslide dams can be hundreds of meters or even thousands of meters, and the ratio of the dam width to the height is small, contributing to a low hydraulic gradient from the dam upstream to downstream sides (Shen et al., 2020). Therefore, seepage failures do not often develop in landslide dams. Nevertheless, seepage has a significant impact on the process of overtopping failure due to the hydraulic gradient from dam upstream to downstream (Gregoretti et al., 2010; Jiang et al., 2019).

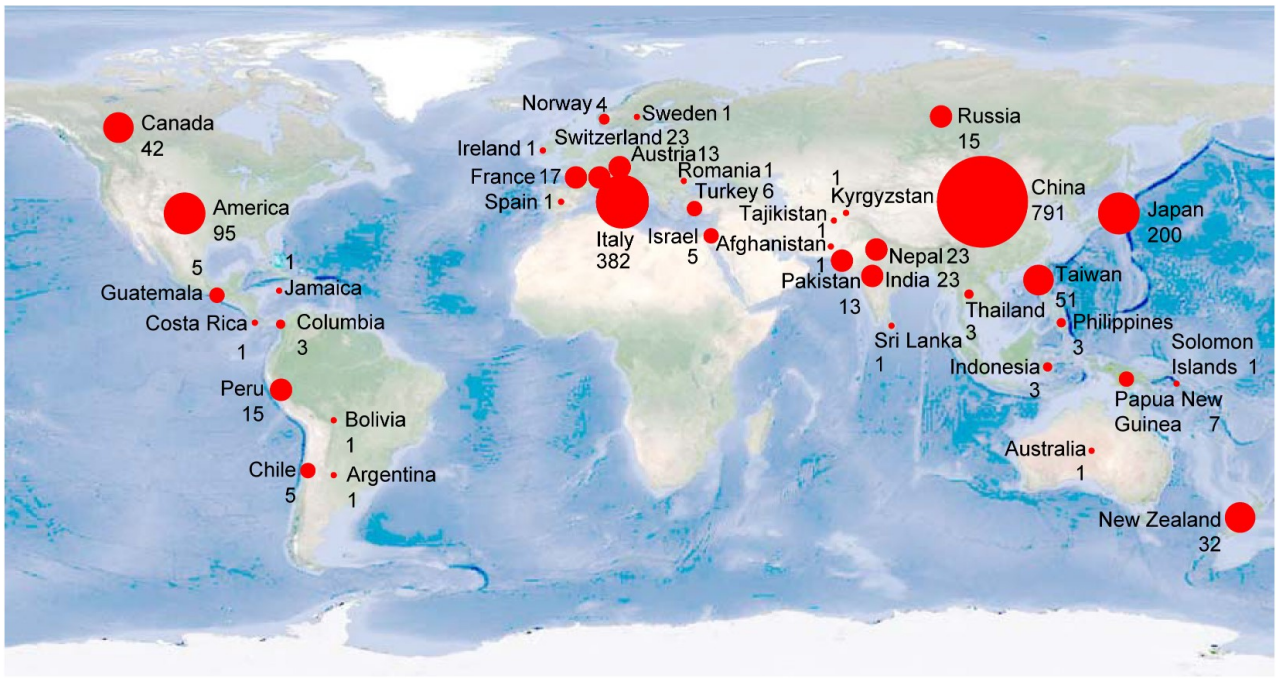

FIGURE 1 | Landslide dam distribution around the world. Red circles denote the proportion of landslide dams and the numbers are the total numbers of landslide dams in each country.

Single-Factor Analyses of Landslide Dam Stability

Landslide dam stability is influenced by various parameters. According to case analyses in the literature (Costa and Schuster, 1988; Casagli et al., 2003), the triggers of slope failures and accumulated materials affect landslide dam stability. The geomorphic parameters characterizing both the dam and the blocked river channel also have an influence on the dam stability (Pirocchi, 1992; Casagli and Ermini, 1999). Based on the compiled landslide dam database, the effects of a single parameter on landslide dam stability are discussed below.

Landslide Dam Triggers

Landslide dams are triggered by earthquakes, rainfall, snowmelt, volcanic eruptions, and other factors (Shi et al., 2014). Most landslide dams are caused by earthquakes and rainfall; 50.4% of landslide dams (700 cases) are induced by earthquakes and 39.3% of landslide dams (546 cases) are caused by rainfall, as shown in **Figure 4A**.

In general, 65% of landslide dams cannot remain stable as shown in **Figure 4B**. Compared with landslide dams induced by earthquakes and other factors, a higher proportion of dams induced by rainfall and snowmelt are unstable: 67.4 and 66.7%, respectively. This trend is consistent with the landslide dams inventoried by Stefanelli et al. (2015) that indicate dam failures caused by intense rainfall and snowmelt make up 53 and 60% of the failures, respectively. It is speculated that the inflow rate of the backwater lake is larger when accompanied by rainfall and snowmelt, resulting in a higher flow velocity and erosion rate during the breach process. Moreover, the water content of landslide dams is high and the material strength of the wet dams is lower than that of relatively dry dams (Nian et al., 2018). Both of these factors could reduce the stability of a landslide dam.

Landslide Dam Material

The material composition of landslide dams could be divided into soil, debris, and rock (Liu et al., 2016). As shown in **Figure 5A**, the proportion of soil-type landslide dams among the inventoried landslide dams is the smallest (21%). The proportion of soil-type landslide dams that are unstable is higher than for the rock and debris types, reaching nearly 80%. Rock-type landslide dams maintain stability better than soil-type and debris-type dams.

Rock-type landslide dams are induced by concordant, discordant, or oblique failures at bedding, jointing, and other contact or bedrock structures (Cui et al., 2009). The Xiaojiaqiao landslide dam was a typical case of rock-type, which had a sliding surface along a bedding-parallel fault with a slickenside and a gouge with a thickness of a few centimeters in carbonate rock (Chigira et al., 2010). As a result of high material strength and stability, blasting was explored to reduce the potential risk of a backwater lake.

Debris-type landslide dams, which are the most prevalent among the inventoried dams (**Figure 5A**), are a mixture of soil, rock, coarse grains, and cuttings. These dams either consist of a relatively homogenous mixture of rock and soil or a distribution of these two materials in different zones (Shen et al., 2020). Taking the Tangjiashan landslide dam as an example, the soil was concentrated on the top of the dam and rock was on the

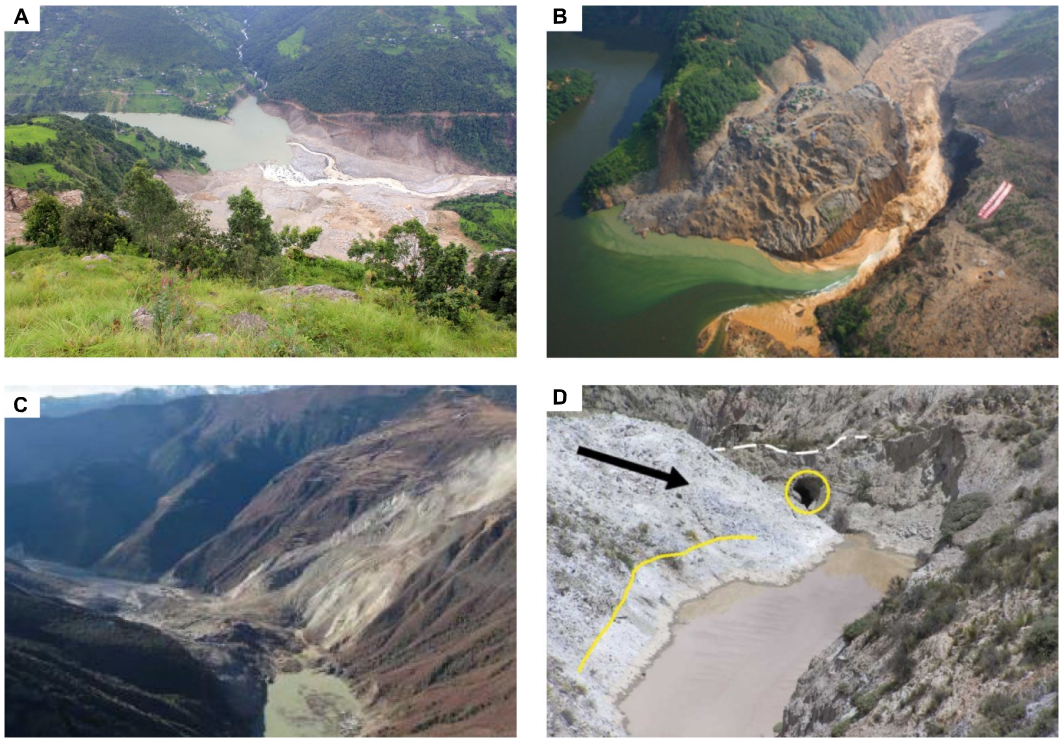

FIGURE 2 | Landslide dam cases. **(A)** Jure landslide dam induced by rainfall in Nepal on September 18, 2014 (Acharya et al., 2016). It was located at 27°46′1.55″N latitude and 85°52′17.10″E longitude. **(B)** Tangjiashan landslide dam induced by an earthquake in China on May 12, 2008 (Peng et al., 2014). It was located at 31°50′24″N latitude and 104°25′48″E longitude. **(C)** Baige landslide dam induced by snowmelt in China on November 3, 2018 (Wang et al., 2020). It was located at 31°04′59″N latitude and 98°42′17″E longitude. **(D)** Allpacoma landslide dam induced by rainfall in Bolivia on July 18, 2004 (Quenta et al., 2007). Overtopping failure occurred for Jure, Tangjiashan, and Baige landslide dams, whereas seepage failure occurred for Allpacoma landslide dam.

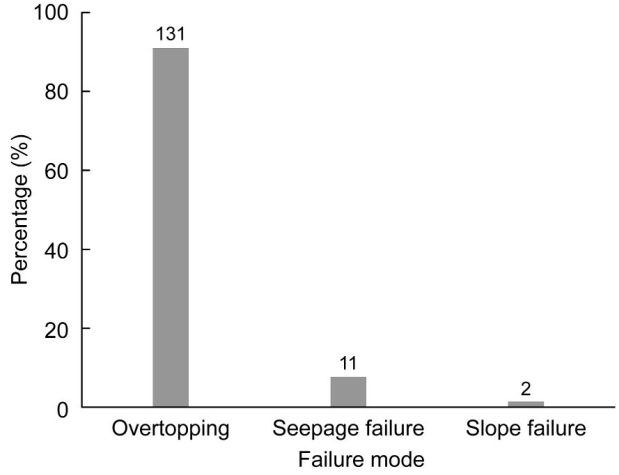

FIGURE 3 | Proportion of landslide dams failed by overtopping, seepage, or downstream slope slide.

bottom. The breaching process ceased when erosion induced by an outburst flooded into the rock layer (Peng et al., 2014).

Soil-type landslide dams are mostly caused by the failure of shallow slopes consisting of colluvium deposit, weathered sediment, loess, man-made fill, or materials displaced from previous man-made construction (Cui et al., 2009). Generally, this type of landslide dam has a low material strength and high erodibility. Taking the Hsiaolin landslide dam as an example, this landslide dam lasted less than 1 h, and it only took approximately 8 min to completely breach due to its low soil strength (Li et al., 2011). This situation also arose for the New-Street soil-type landslide dam (Cui et al., 2009).

Geomorphic Characteristics

The geomorphic characteristics of landslide dams could be categorized as geometric and hydrological parameters. Peng and Zhang (2012) define these parameters as shown in **Table 1**. The geometric parameters are summarized as the dam height, dam length, dam width, and dam volume. The hydrological parameters are listed as the inflow rate and lake volume.

It is commonplace that the geometric parameters of landslide dams cannot be obtained immediately with field investigations due to their remote locations. Fan et al. (2012) employed post-landslide remote sensing images and the pre-landslide digital terrain model in the geographic information system (GIS) to estimate the geomorphic characteristics. This method has also been adopted by Kuo et al. (2011) and Dong et al. (2014). While the dam height, dam length, and lake volume could be obtained by GIS, the dam width in the upstream direction is difficult to

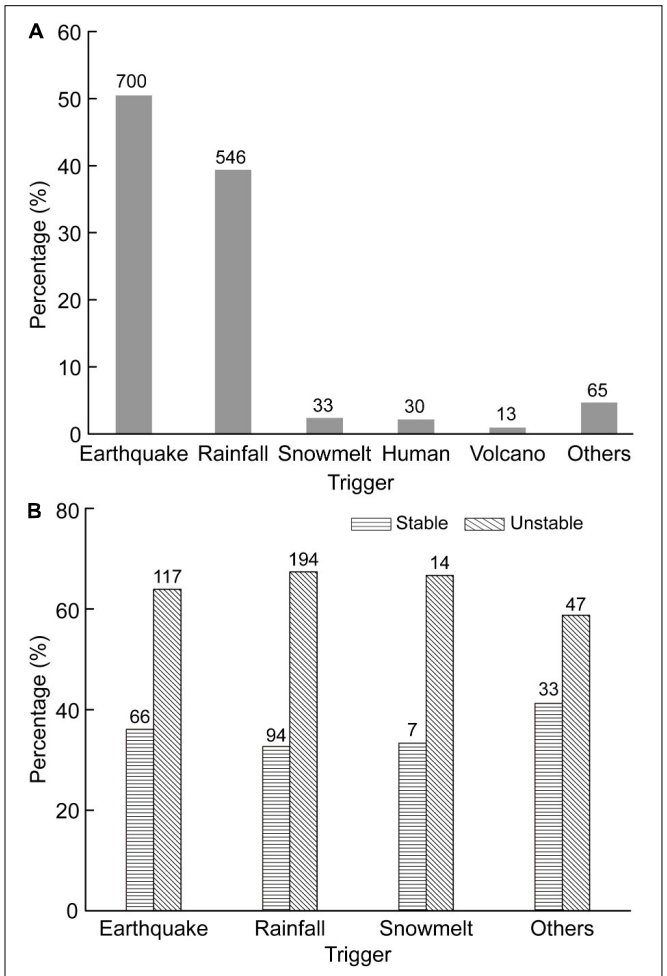

FIGURE 4 | Effects of landslide dam trigger on the stability: **(A)** landslide dam triggers and **(B)** landslide dam stability.

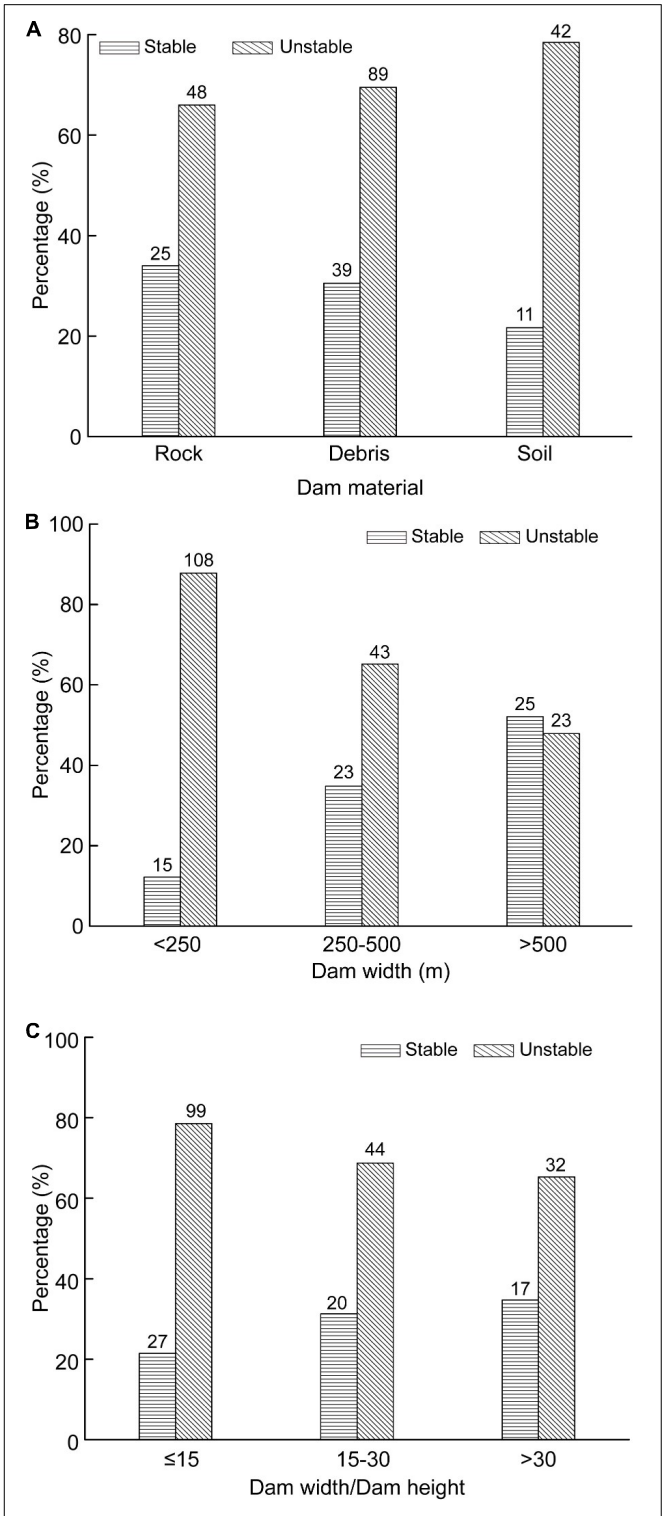

FIGURE 5 | Effects of **(A)** dam material, **(B)** dam width, and **(C)** the ratio of dam width to dam height on landslide dam stability.

determine from a satellite image because of the water stored in the backwater lake (Kuo et al., 2011).

Dam width and dam height

Landslide dam stability increases with increasing dam width and the ratio of the dam width to the dam height as shown in **Figures 5B,C**. The proportion of failed landslide dams with dam widths smaller than 250 m is 88%, compared to 48% for landslide dams with dam widths larger than 500 m. The proportion of failed landslide dams for which the ratio of the dam width to the dam height is smaller than 15 is 87%, which reduces to 65% for landslide dams with a ratio of the dam width to the dam height larger than 30.

From a physical point of view, the dam height and dam width are important parameters to assess landslide dam stability against both overtopping and seepage failures. For the former, they determine the steepness of the dam slope downstream and the corresponding flow velocity and erosion ability of the overtopping waters. For the latter, they control the elevation of the water table through the landslide dam and especially its hydraulic gradient (Ermini and Casagli, 2003).

Dam volume

The global dam stability increases with increasing landslide dam volume (**Figure 6**). The proportions of failed landslide dams

TABLE 1 | Geomorphic characteristics of landslide dams (Peng and Zhang, 2012).

Geometric parameters	Dam height	Vertical altitude difference from the valley floor to the lowest point on the landslide dam
	Dam length	Crest length of the landslide dam measured perpendicular to the major valley axis
	Dam width	Base width of the landslide dam measured parallel to the main valley axis
	Dam volume	Part of landslide volume which blocks the river
Hydrological parameters	Inflow rate	Statistical average annual inflow rate in the studied river
	Lake volume	Volume of water ponded behind the landslide dam
Schematic diagram	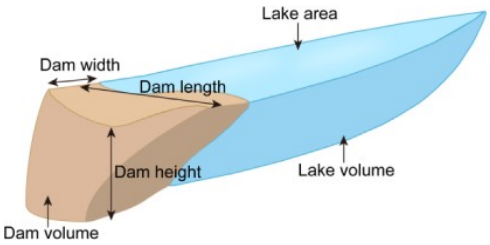	

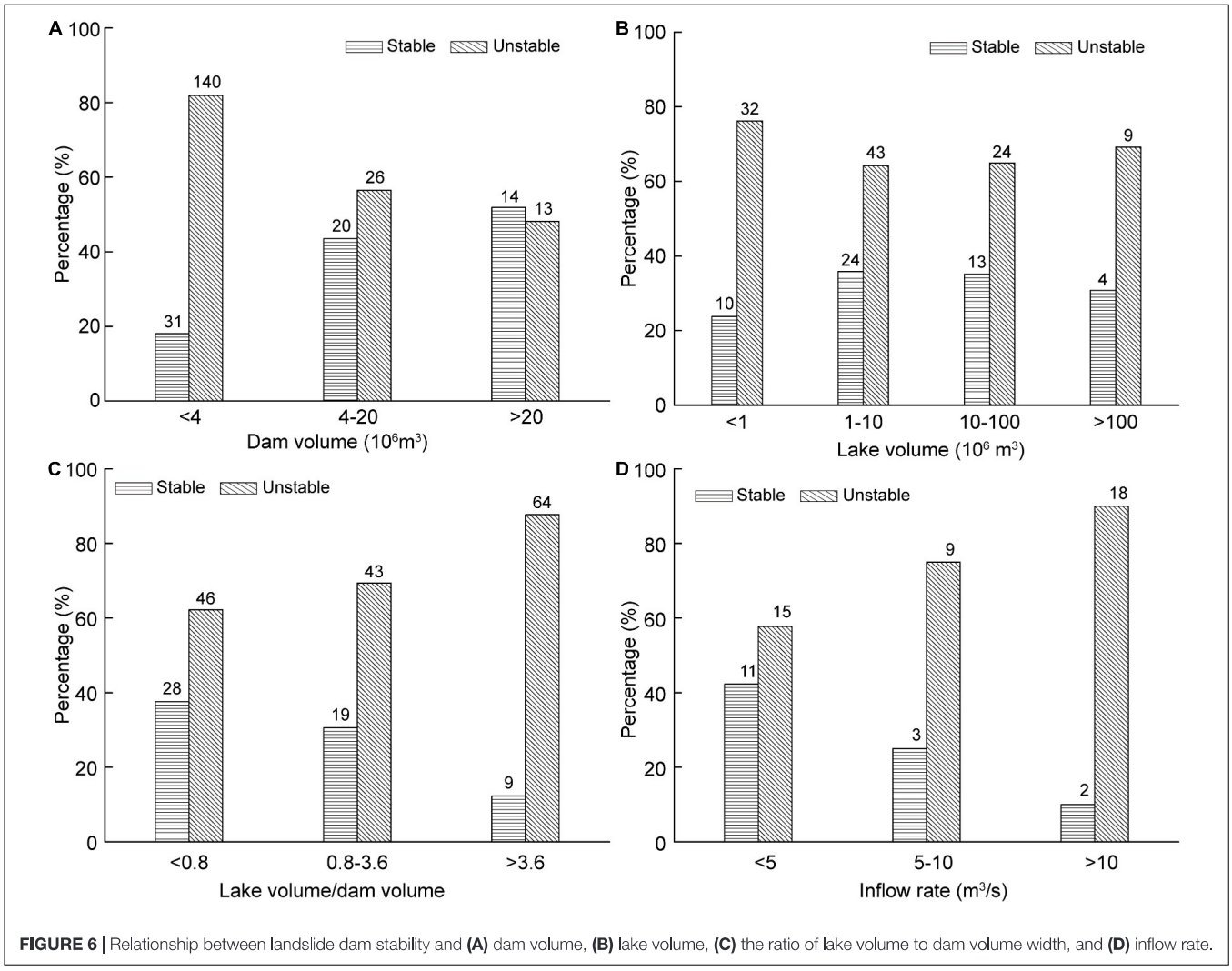

FIGURE 6 | Relationship between landslide dam stability and **(A)** dam volume, **(B)** lake volume, **(C)** the ratio of lake volume to dam volume width, and **(D)** inflow rate.

with dam volumes smaller than 4×10^6 m^3 and larger than 20×10^6 m^3 are 82 and 48%, respectively. The volume could well identify the dam stability by affecting the dam geometry: width, height, and length. Dam volume is always considered as an influencing factor in the assessment indexes of landslide dam stability (Canuti et al., 1998; Ermini and Casagli, 2003).

Evans et al. (2011) present a special review on natural and artificial rockslide dams and conclude that most recorded

dams exceed 1 million m^3 in volume. This also applies to our inventoried landslide dams (**Figure 6**). Whether the landslide volume or landslide dam volume should be selected as the factor influencing landslide dam stability remains controversial. According to Stefanelli et al. (2016), the morphometric data processing of post-landslide dams leads to some errors, proportional to the amount of eroded material. The loss of relative volume and the percentage error are smaller if compared to the total landslide volume rather than to the dam volume.

Lake volume

There is no discernable relationship between landslide dam stability and lake volume (**Figure 6B**). However, landslide dam stability decreases gradually as the ratio of the lake volume to the dam volume increases (**Figure 6C**). According to the statistics, the lake volume does not have a significant correlation with the dam volume (Shen et al., 2020). The lake volume is determined by the dam height and valley geometry. Compared with the lake volume, the catchment area is usually more accessible and often used as the influencing factor in assessment indexes of landslide dam stability (Ermini and Casagli, 2003; Stefanelli et al., 2016).

A stable landslide dam in New Zealand would require a 10-fold dam volume for a given lake volume (Korup, 2004). Nevertheless, some landslide dams among our inventoried landslide dams remain stable even though the lake volume is larger than the dam volume. For example, the Val Pola landslide dam in the Adda River is still stable due to a large dam width of 2.5 km (Crosta et al., 2004).

Inflow rate

There is a negative correlation between landslide dam stability and the inflow rate as shown in **Figure 6D**; 42% of landslide dams cannot remain stable when the inflow rate is smaller than 5 m^3/s. Due to overtopping, landslide dams do not usually remain stable when the annual average inflow rate is larger than 10 m^3/s. Some ancient landslide dams could exist for centuries with a small inflow rate from weak precipitation, and they are currently used for recreation and tourism, such as Valasht lake (Ehteshami-Moinabadi and Nasiri, 2019) and Sarez lake (Schuster and Alford, 2004).

The inflow rate of a landslide dam caused by rainfall and snowmelt is normally higher than the annual average river discharge, leading to a lower landslide dam stability. For example, the inflow rate at the blockage of the Hsiaolin landslide was 2,974 m^3/s (Dong et al., 2011): significantly larger than the annual average inflow rate (30 m^3/s). However, the actual inflow rate during the period of landslide dam formation is not usually recorded in historical cases, and thus, the average flow rate in the studied river is chosen to take its place (Shen et al., 2020).

Multifactor Analyses of Landslide Dam Stability

Based on the single-factor analyses discussed above, the following three factors are closely related to landslide dam stability: (1) the backwater lake; (2) the dam geometry; and (3) the dam material. Currently, the geomorphic approach is widely used to correlate the characteristic parameters of the dam and river with the stability of a landslide dam (Costa and Schuster, 1988; Casagli and Ermini, 1999; Ermini and Casagli, 2003; Korup, 2004; Dong et al., 2009). The parameters used in the indexes are all interlinked, and their relative significances are compared to fully evaluate landslide dam stability (Fan et al., 2020).

Canuti et al. (1998) proposed the blockage index (BI):

$$\mathrm{BI} = \log\left(V_d/A_b\right) \tag{1}$$

where V_d is the dam volume (m^3) and A_b is the upstream basin area at the point of blockage (km^2). BI reflects the contributions of the landslide volume and the drainage basin area to the stability of a landslide dam (Swanson et al., 1986).

Considering the dam height in the equation, Ermini and Casagli (2003) proposed a different formulation, the Dimensionless BI (DBI):

$$\mathrm{DBI} = \log\left(A_b H_d/V_d\right) \tag{2}$$

where H_d is the dam height (m). According to their study, the dam height is an important parameter to assess landslide dam stability against both overtopping and seepage failures. It influences the downstream slope in an overtopping failure and the hydraulic gradient in a piping failure (Ermini and Casagli, 2003). The DBI was obtained by analyzing 84 landslide dam cases. The two limits identifying the different domains were DBI = 2.75 for the stability domain and DBI = 3.08 for the instability domain (Ermini and Casagli, 2003). Chen et al. (2017) applied the DBI to assess the Attabad landslide dam stability: its DBI was 4.62–4.85 which confirmed the instability of the dam.

Based on the dam height, Korup (2004) proposed three dimensionless indexes: the Backstow index I_s, Basin index I_a, and Relief index I_r.

$$\mathrm{I_s} = \log\left(H_d^3/V_l\right) \tag{3}$$

where V_l is the lake volume. The values of $I_s < -3$ and $I_s > 0$ delimited the stable and unstable landslide dam domains, respectively.

Similarly, $\mathrm{I_a} = \log\left(H_d^2/A_b\right)$. A landslide dam would be stable with $I_a > 3$.

The relief index I_r is expressed as follows:

$$\mathrm{I_r} = \log\left(H_d/H_b\right) \tag{4}$$

where H_b is the relief upstream of the point of blockage. $I_r = -1$ is used to distinguish stable from unstable landslide dams.

Considering dam destabilization by the river using a simplified expression of stream power ($A_b S$) per unit channel length (where S is the local longitudinal slope of the channel bed), Stefanelli et al. (2016) presented the hydromorphological dam stability index (HDSI):

$$\mathrm{HDSI} = \log\left(V_L/\left(A_b S\right)\right) \tag{5}$$

where V_L is the landslide volume. Kumar et al. (2019) forecasted the damming process of the Urni landslide and employed the HDSI and DBI indexes to evaluate the stability of the potential landslide dam.

The above geomorphometric parameters do not consider the effect of the dam material on the stability. Based on the DBI, the

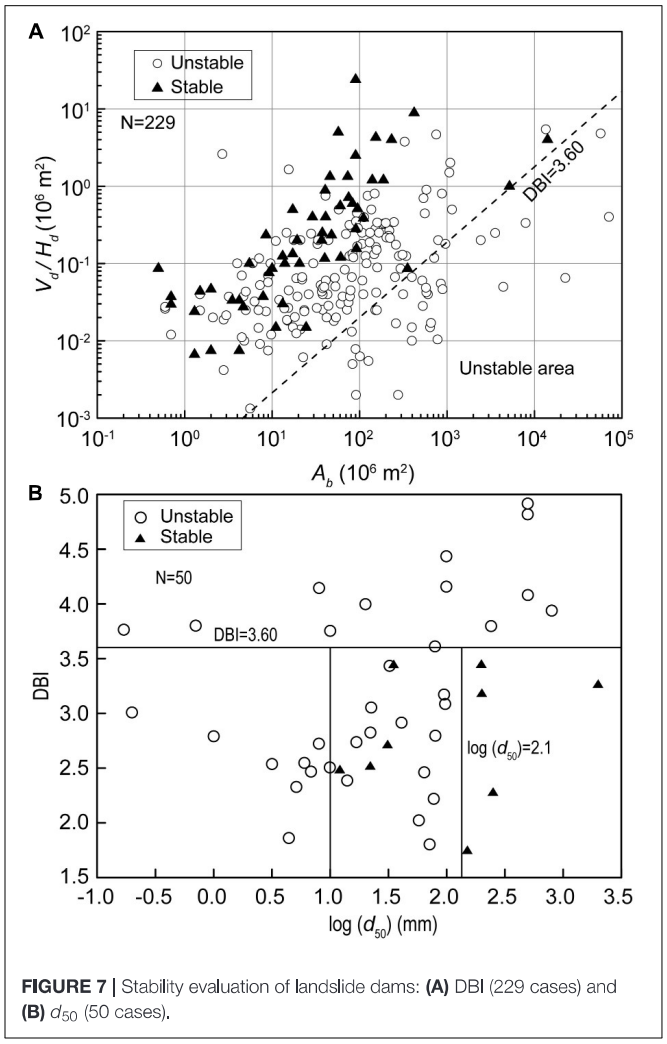

FIGURE 7 | Stability evaluation of landslide dams: **(A)** DBI (229 cases) and **(B)** d_{50} (50 cases).

landslide dam stability is further discerned by use of the median particle size d_{50}. The DBI was calculated by examining 229 landslide dam cases as shown in **Figure 7A**. A landslide dam was unstable with DBI > 3.6, whereas the data above this envelope remained inconclusive. Fifty landslide dams (**Supplementary Appendix 1**) with their grain compositions were extracted from these 229 cases. Three different domains of existence could be recognized (**Figure 7B**), as follows:

> Unstable domain, log (d_{50}) < 1.0. Below this threshold value, the dam materials mainly consist of debris grains smaller than 10 mm and have a marked tendency to erode. Therefore, the landslide dams are unstable.
> Uncertain domain, 1.0 < log (d_{50}) < 2.1. In this domain, the grain size distribution of the dam material is uncertain. It may be a gap-graded mixture or may be dominated by the median particle size, which makes it difficult to determine the landslide dam stability.
> Stable domain, log (d_{50}) > 2.1. Above the threshold value, the dam materials mainly consist of gravel and cobble with a high anti-erosion ability.

The database of landslide dam cases is used to test various evaluation indexes as shown in **Table 2**. It is difficult to discern the stability of a landslide dam using BI and I_s. I_a has an advantage to predict the instability of landslide dams. On the whole, DBI can be used to predict the stability and instability of landslide dams with an accuracy of approximately 60%. The prediction of landslide dam instability can be further improved by considering the dam materials.

STABILITY ANALYSES OF SPECIAL FACTORS ON LANDSLIDE DAMS

The stability of a landslide dam is determined not only by geomorphometric parameters, but also by special factors including aftershocks, surges, and engineering mitigation measures. These are discussed individually below.

Stability Analysis of Aftershocks on Landslide Dams

Landslide dams triggered by earthquakes are always subjected to many aftershocks. After the Wenchuan earthquake, more than 300 aftershocks with magnitudes higher than *Ms* 4.0 occurred after the formation of these landslide dams (Shen et al., 2013), which might significantly influence the soil properties and structures of these dams.

The effects of seismic action on embankment dams have been widely studied (Chen and Harichandran, 2001; Proulx et al., 2001; Wu, 2001; Swaisgood, 2003; Calayir and Karaton, 2005; Arabshahi and Lotfi, 2008; Chen et al., 2008; Bilici et al., 2009; Sevim et al., 2011; Zou et al., 2013). The stress concentration, soil liquefaction, ground deformation, and crushing damage in the zone of the slabs are the common failure patterns for embankment dams. These failure patterns are rarely observed for landslide dams due to the different dam materials and morphological characteristics.

A series of large-scale shaking table tests were conducted to investigate the dynamic behavior of landslide dams under various aftershocks (Shi et al., 2015b,c). Videogrammetry was employed to measure the dynamic deformation of the model dams. The seismic actions gave rise to settlements and horizontal deformations in the landslide dams due to loosened dam material. The settlements increased from the dam bottom to the dam crest. The displacements close to the slope surface of the dam were larger than those in the interior. Higher peak ground acceleration led to larger dam deformations due to higher seismic forces. Aftershocks may not directly lead to dam failure, but the cracks and settlements caused by the aftershocks may accelerate dam failure, accompanied by overtopping as shown in **Figure 8**.

Stability Analysis of Surges on Landslide Dams

The rising water level in backwater lakes may induce a series of landslides or avalanches (Xu et al., 2017). In addition, debris flows possibly migrate out of a gully and slide into a lake area (Hu et al., 2009). When a landslide or debris flow quickly rushes

TABLE 2 | Evaluation indexes for landslide dam stability.

Investigators	Cases	Indexes	Stability area	Accuracy (%)	Instability area	Accuracy (%)
Casagli and Ermini, 1999	255	$BI = \log\left(\frac{V_d}{A_b}\right)$	BI > 5	_	3 < BI < 4	_
Ermini and Casagli, 2003	243	$DBI = \log\left(\frac{A_b H_d}{V_d}\right)$	DBI < 2.75	61	DBI > 3.08	62
Korup (2004)	203	$I_s = \log\left(\frac{H_d^3}{V_l}\right)$	$I_s > 0$	4	$I_s < -3$	13
Korup (2004)	243	$I_a = \log\left(\frac{H_d^2}{A_b}\right)$	$I_a > 3$	0	$I_a < 3$	56
Present paper	229	DBI+d_{50}	DBI < 3.6 and log (d_{50}) > 2.1	56	DBI > 3.6 or log (d_{50}) < 1.0	76

BI obtained from 255 landslide dams presented in the paper is smaller than 1.0 and it lies outside of the criteria proposed by Casagli and Ermini (1999).

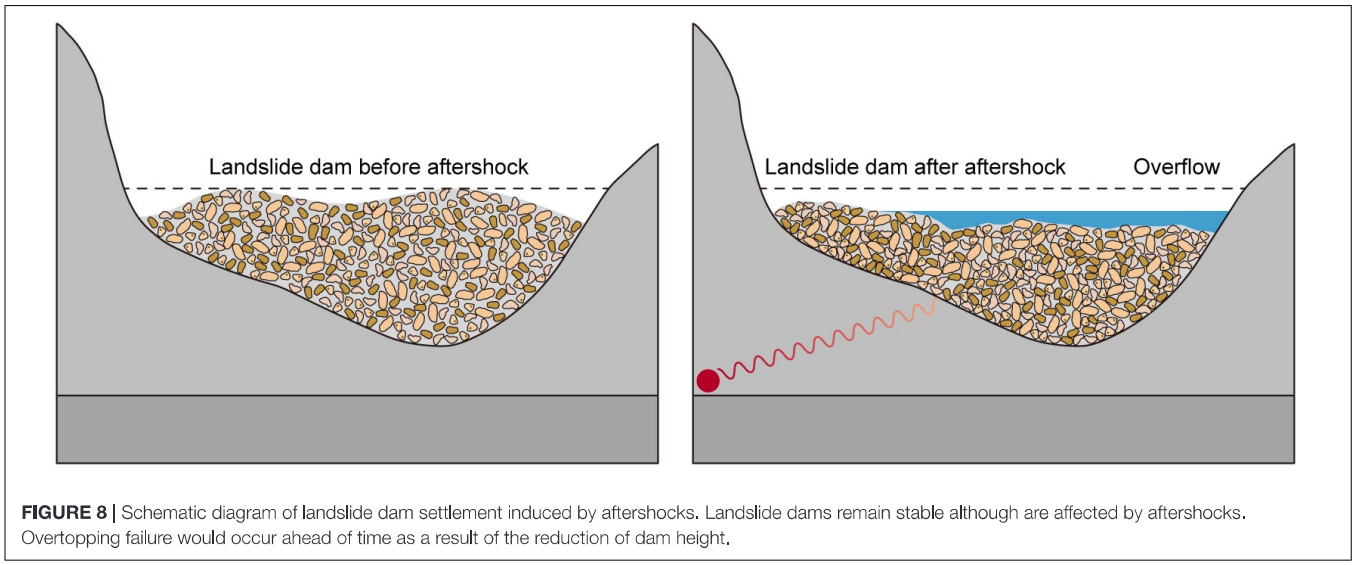

FIGURE 8 | Schematic diagram of landslide dam settlement induced by aftershocks. Landslide dams remain stable although are affected by aftershocks. Overtopping failure would occur ahead of time as a result of the reduction of dam height.

into a reservoir, it may result in huge surge waves (Hager et al., 2004; Koo and Kim, 2008). For example, a landslide of 300 million m^3 rapidly slid into the Vaiont Reservoir in Italy in 1963, and an enormous surge with a wave height as high as 300 m was generated (Tang and Lee, 1992). A glacial avalanche rushed into a moraine lake with a volume of 6.5 million m^3 in Nastetuku River, Canada, in 1983, and the moraine dam was completely breached in less than 5 h under the impact of large surge waves (Risley et al., 2006).

The surges can significantly erode a landslide dam and reduce its width and height, causing more rapid overtopping failures than under normal conditions. The surge scale increases with an increase of the contact area between a landslide and the water surface and landslide height, directly reducing the stability of a landslide dam. Nevertheless, the effect of the distance from the entry point of a landslide to the dam site on the surge wave is limited (Wiegel, 1970; Xu et al., 2015). In addition, dynamic water pressure caused by the surge wave is applied on the upstream slope of a landslide dam (Chen H.Y. et al., 2015). The maximum pressure load increases with increasing sliding distance and significantly reduces the landslide dam stability by diminishing the effective stress.

As shown in **Figure 9**, the failure process of a landslide dam caused by a surge could be generalized as a three-stage process (Peng et al., 2019). In Stage I, a scour base plane is formed on the upstream slope of a landslide dam. Then, the scour surface intersects with the dam crest and gradually moves downstream under the action of waves. In Stage II, erosion occurs on both the upstream slope by surge waves and the downstream slope by overflow. In Stage III, an inclined erosion slope appears and much more intense erosion occurs during the overtopping process. Then, the erosion gradually slows down, leaving a residual dam behind.

The wave height and water level play different roles during the process of dam failure (Peng et al., 2019). The wave height determines the erosion boundary above the water level, while the water level determines the erosion position on the upstream slope. The landslide dam stability is determined by the difference (ΔH) between the effective water level h_w (the sum of water level h_l and wave height h_h) and the effective dam height h_d (the dam height after reduction due to local erosion and collapse). When $\Delta H < 0$, a stable eroded upstream surface eventually forms; when $\Delta H > 0$, the dam is overtopped and fails under the action of the subsequent wave loadings (**Figure 9**).

Stability Analysis of Engineering Mitigation Measures on Landslide Dams

If a landslide dam has a high tendency to fail, engineering mitigation measures might be employed to stabilize the blockage or accelerate its failure to reduce the potential risk (Chen et al., 2011). Yang et al. (2010) and Cui et al. (2012) introduced the

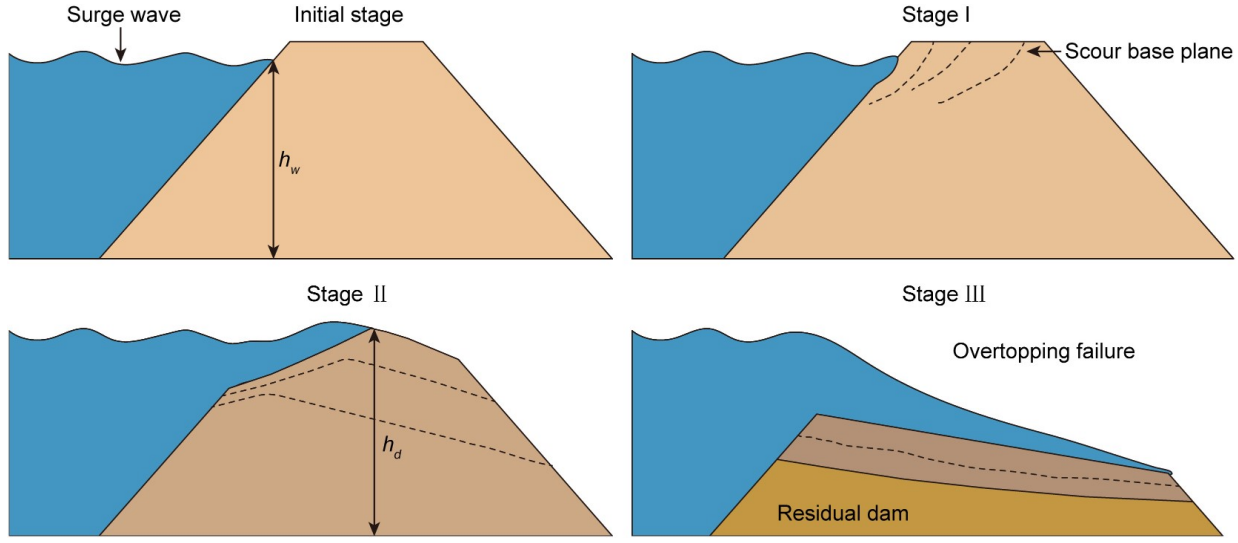

FIGURE 9 | Scouring failure process of a landslide dam by a surge wave. h_w and h_d are the effective water level and effective dam height, respectively.

experiences of handling some landslide dams induced by the Wenchuan earthquake. Schuster and Evans (2011) summarized the mitigation measures employed for 20 historical cases. Sattar and Konagai (2012) presented hazard-mitigation strategies for several large landslide dams. These measures could be categorized into short-term and long-term measures (Peng et al., 2014).

Short-term measures consist of diversion, drainage, and control of the erosion rate during overtopping failure. These measures are a temporary approach to control a landslide dam's stability. Diversion or drainage could be employed to stabilize the dam by controlling the rising reservoir level when surrounding hydraulic facilities, such as a reservoir, siphon, and pump, are available. This allows time to build the long-term measures. For example, diversion was applied to the Randa landslide dam formed in 1991 in the Vispa River, Switzerland, and a spillway across the dam was then constructed (Bonnard, 2004). Pumps were installed at the Higashi Takezawa landslide dam, and a 280-m-long concrete-faced spillway was then constructed (Sattar and Konagai, 2012). However, some measures may be used to accelerate a dam's instability to prevent continuous rising of the reservoir level. For example, excavation and blasting were employed for the Yanziyan landslide dam to eliminate large rocks to hinder further overtopping failure (Li et al., 2008).

Long-term measures consist of drainage tunnels, spillways, and drainage conduits. These long-term measures are conducive to controlling the reservoir water level and are fundamental approaches to maintain the stability of the landslide dam. The Hongshiyan landslide dam triggered by the Ludian earthquake is a typical example (Shi et al., 2017). An existing drainage tunnel connecting the hydropower plant and reservoir became a diversion channel for the landslide dam. Spillways and drainage conduits are easier and cheaper to construct than drainage tunnels. Limited by available time and transportation facilities, constructed spillways are commonly designed to reduce the water level of the backwater lake rather than to serve as permanent structures (Peng et al., 2014). However, not all spillways are successful in preventing rapid overtopping failures. For example, the peak flow rate of the Yigong dam after constructing a spillway 1,000 m long, 24 m deep, and 150 m wide on the top and 20 m wide on the bottom was still as high as 124,000 m^3/s (Shang et al., 2003).

OVERTOPPING FAILURE ANALYSES OF LANDSLIDE DAMS

Experimental Analyses of Overtopping Failures of Landslide Dams

Model experiments on the overtopping failures of landslide dams are valuable to gain more insight into the development process of dam failures and to calibrate and validate of the corresponding numerical models described below (Zhu et al., 2004).

Homogenous sand or gravel are currently considered as the model dam materials (Javadi and Mahdi, 2014; Jiang and Wei, 2019; Liu et al., 2019). The silt and sand components below 1 mm are always excluded due to their cohesive properties, resulting in a complex overtopping failure mechanism (Schmocker and Hager, 2009). Cao et al. (2011b) observed that cohesive clays may act to mitigate seepage through the dam, and the gravel in the dam could appreciably depress the rate of the dam failure process. This is consistent with the observation of large-scale model experiments by Morris et al. (2007) and Zhong et al. (2019). In contrast, coarser grains lead to a faster breach process compared with finer materials as indicated by Pickert et al. (2011). The reason proposed for the difference is that negative pore-water pressure is generated in the finer material with the apparent cohesion (Pickert et al., 2011). The grain size distributions (grain diameter greater than 0.75 mm) have a small effect on the overall overtopping failure process and no increased

erosion resistance is observed for the soil mixtures (Schmocker et al., 2014). The results show that the mean grain diameter adequately describes the non-cohesive material characteristics and general overtopping failure features at laboratory scale can be investigated using uniform material.

According to the specifics of the breach process, overtopping failure can be divided into various stages (Chen R. et al., 2015). The overtopping failure process could be described as initial downstream surface erosion progressing to stair-stepped multiple overfalls, ultimately merging into a single upstream-migrating headcut (Hanson et al., 2002). Kakinuma and Shimizu (2014) categorized the overtopping failure process into the following four stages: downstream slope erosion, breach widens gradually, overflow rate increases significantly, and breach rate decreases. By comparing the field data with the overtopping erosion process, the final phase of overtopping erosion is overestimated. An armor layer appears on the downstream slope during the final stage of breach development in centrifugal model tests (Zhao et al., 2018, 2019).

Commonly, the cross section of the breach during the overtopping process is considered as triangular, rectangular, trapezoidal, or parabolic (Fread, 1988; Pickert et al., 2011; Peng et al., 2014). The predominant presumption of a trapezoidal breach cross-section is based on observations of final breach shapes, like Tangjiashan and Xiaogangjian landslide dams (Chang and Zhang, 2010). However, the final breach shape is influenced by falling reservoir water levels and therefore does not represent the breach shape during the breach event (Coleman et al., 2002). Breach side walls are typically vertical and even overhanging during breach development (Morris et al., 2007; Pickert et al., 2011).

The overtopping failure patterns can be summarized as four types through the existing model experiments as shown in **Figure 10**. For Case (a), the downstream slope angle rapidly increases until a constant critical soil friction angle is achieved; thereafter, the angle is maintained to breach end (Guan, 2018). This model is consistent with the theoretical model reported by Powledge et al. (1989). For Case (b), the breach channel initially erodes the downstream face of the dam with an inverted slope parallel to the face; then, the breach inverted slope progressively flattens to a terminal value by rotating about a fixed pivot point along the dam base (Coleman et al., 2002; Schmocker and Hager, 2009). For Case (c), the channel first develops a stepped profile and the upstream migration of the steps coalesces into a headcut. Thereafter, the retreating headcut maintains a slope near the internal friction angle of the dam material (Walder et al., 2015). For Case (d), the erosion point moves from the downstream dam crest toward the upstream dam crest and the dam toe. Then, a spindle-like failure process is observed along the flow direction (Zhou G.G.D. et al., 2019; Zhou M. et al., 2019).

The overtopping failure patterns are affected by various factors including the lake volume, downstream slope, and dam material. Compared with Cases (a) and (b), the lake volume is relatively small in Case (b), and the entrainment capacity is drastically reduced with the release of the lake volume during the failure process, resulting in a progressive flattening of the slope. The landslide dam is located in the flume with a large longitudinal slope in Case (d) (Zhou G.G.D. et al., 2019), whereas the flumes are horizontal in Cases (a), (b), and (c). As a result of a larger bed slope, the erosion stress and entrainment power of a beaching flood are larger in Case (d), leading to rapid erosion close to the crest. The dam materials in Cases (a) and (c) are fine-grained soils and the lake volumes are comparatively large; thus, a slope near the internal friction angle of the dam material could be maintained. The stepped profile in Case (d) is caused by the hydraulic jump when a breaching flood flows through the dam crest and downstream slope of the dam (Walder et al., 2015).

Multiple landslide dams triggered by strong shock or rainstorm are usually closely distributed along river reaches or gullies (Shi et al., 2015a). The outburst flood released by a landslide dam upstream can induce failures of downstream landslide dams one after another. Compared with a single landslide dam, the impact of cascading landslide dam failures is more complicated (Zhou et al., 2013). For instance, Tangjiashan landslide dam and two other dams downstream (Shi et al., 2015a) as well as Xiaogangjian and Yibadao landslide dams (Niu et al., 2012) breached in succession. At least 19 landslide dams in the Sanyanyu gully were destroyed by upland flash floods and developed into a catastrophic debris flow in Zhouqu (Cui et al., 2013). The breach of cascading landslide dams may result in a sharp increase in the peak outflow rate and a more rapid breach process of any downstream dam (Cao et al., 2011a). In addition, multi-peak floods are very likely to develop at a downstream landslide dam, due to the overlapping effect of breach discharges upstream and downstream (Shi et al., 2015a). However, similarities and differences in the breach processes and failure patterns of single and cascading landslide dams are still unclear.

Numerical Analyses of the Overtopping Failure of Landslide Dams

To enable early warning and reduce risks and losses, it is absolutely necessary to develop a numerical model to predict the overtopping failure process of landslide dams (Peng and Zhang, 2013; Chen et al., 2017). Generally, the numerical models of overtopping failures of landslide dams can be classified as physically based models or coupled shallow water hydrodynamic models.

Physically Based Models

Physically based models adopt the principles of hydraulics, soil mechanics, and sediment erosion to calculate time-stepping solutions of the growth process of dam failure and the outflow hydrograph. Typical models of this type include BREACH (Fread, 1988; Fujisawa et al., 2009) and its modified models (Mohamed et al., 2002; Morris et al., 2009), BEED (Singh and Scarlatos, 1988), and BRES (Loukola and Huokuna, 1998). These models are widely employed to investigate overtopping failures of embankment dams. The geometrical parameters of the dam and initial breach as well as the material strength such as cohesion and internal friction angle are required before iterative calculation.

Compared with the abovementioned models, some modified models, such as DABA (Chang and Zhang, 2010), DB-IWHR (Chen Z.Y. et al., 2015; Zhong et al., 2018), and

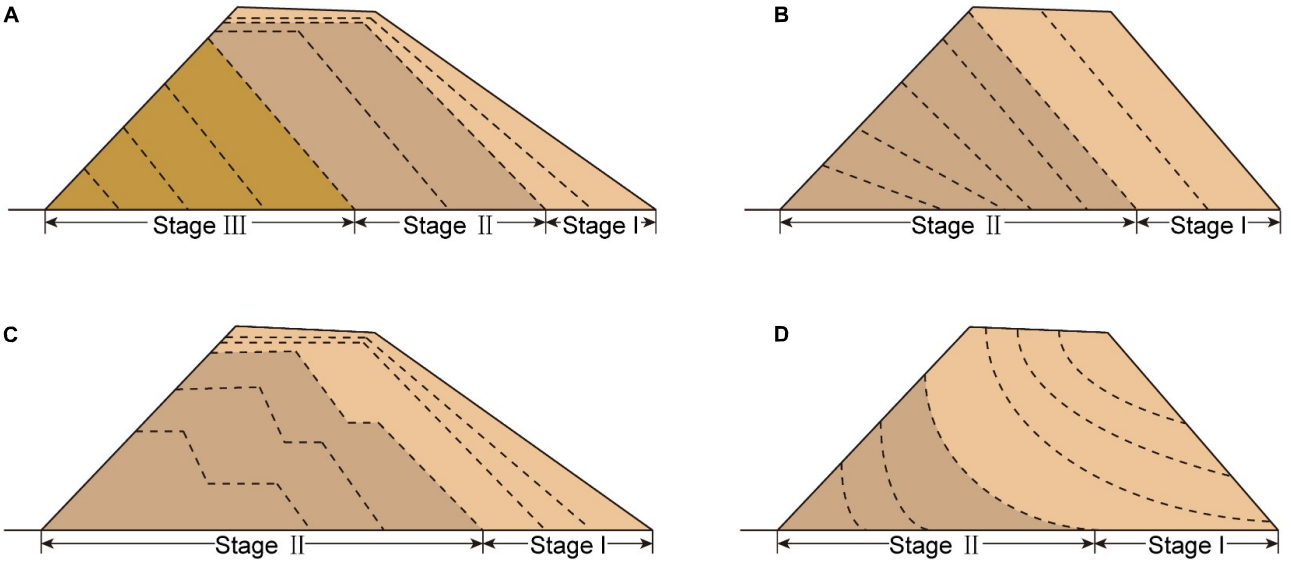

FIGURE 10 | Overtopping failure patterns of landslide dams: **(A)** downstream slope angle rapidly increases until a constant critical soil friction angle is achieved and then the angle is maintained to breach end; **(B)** downstream dam face is initially eroded with an slope parallel to the face, then the breach inverts slope, progressively flattening to a terminal value; **(C)** a stepped profile is first developed and then the retreating headcut maintains a slope near the internal friction angle of the dam material; and **(D)** a spindle-like failure process is observed along the flow direction.

DLBreach (Wu and Li, 2017), have been developed to analyze the overtopping failure process of landslide dams. The dam material is commonly assumed to be uniformly distributed along the depth for homogeneous embankment dams (**Figures 11A,B**). However, for a landslide dam, the erodibility changes significantly from the dam crest to the native foundation due to changes in the soil type, density, and grain composition (Chang et al., 2011). Variations in the soil erodibility along the depth are thus considered in the DABA model. The erosion processes of Tangjiashan and Xiaogangjian landslide dams have been successfully simulated by using the DABA model. Commonly, the lateral banks are assumed to uniformly widen (**Figures 11C,D**). If the slope stability of the lateral banks is considered, bank erosion occurs only within the water area at the initial stage. The lateral banks undergo undercutting by the breaching flood and the debris soil on the lateral banks above the water surface slides down to the breach bottom at a critical slope (Chen Z.Y. et al., 2015; Zhong et al., 2018). For the cascading breach of landslide dams or surge wave in the backwater lake, the sudden increase in the inflow rate would cause erosion both within and outside of the breach (Shi et al., 2015a; Wu and Li, 2017). The erosion on the dam crest and breach should be considered, and the overflow discharge outside and within the breach should be combined as the total outflow discharge (**Figures 11E,F**).

Coupled Shallow Water Hydrodynamic Models

Coupled shallow water hydrodynamic models are based on the mass conservation equations for the sediment and dam material, and the mass and momentum conservation equations for the water–sediment mixture flow (Cao et al., 2011c). This method has been widely employed to investigate the overtopping failure process (Huang W. et al., 2014; Chen S.C. et al., 2015; Do et al., 2016; Zheng et al., 2016; Liu and He, 2018; Wang, 2018; Wu and Lin, 2019). The calculation cost of coupled shallow water hydrodynamic models is significantly larger than that of physically based models due to the solution of conservation equations. Nevertheless, the former class of models offers a higher spatial resolution. To consider sediment transport and bed morphological evolution, a double layer-averaged model has been proposed by Li et al. (2013) and Ouyang et al. (2014). The influences of seepage flow through the dam material on the apparent cohesion and overtopping failure initiation have been investigated (Volz et al., 2017). In recent years, some novel solution algorithms and graphics processing units (GPUs) have been employed to achieve speedups of up to two orders of magnitude (Dazzi et al., 2019). This is very beneficial for predicting the overtopping failure processes of landslide dams with large volumes.

In addition, other computational fluid dynamics methods are also used to investigate overtopping failure of landslide dams like the smoothed particle hydrodynamics (SPH) approach (Memarzadeh et al., 2018) or discontinuous deformation analysis (DDA) coupled with SPH method (Wang M. et al., 2017). Two-phase formulations are used in the SPH numerical algorithms to examine the free surface and bed evolution profiles, in which the entrained sediments are treated as a different fluid component (Ran et al., 2015). Compared with these numerical methods, coupled shallow water hydrodynamic models offer the advantage of high computational efficiency. This

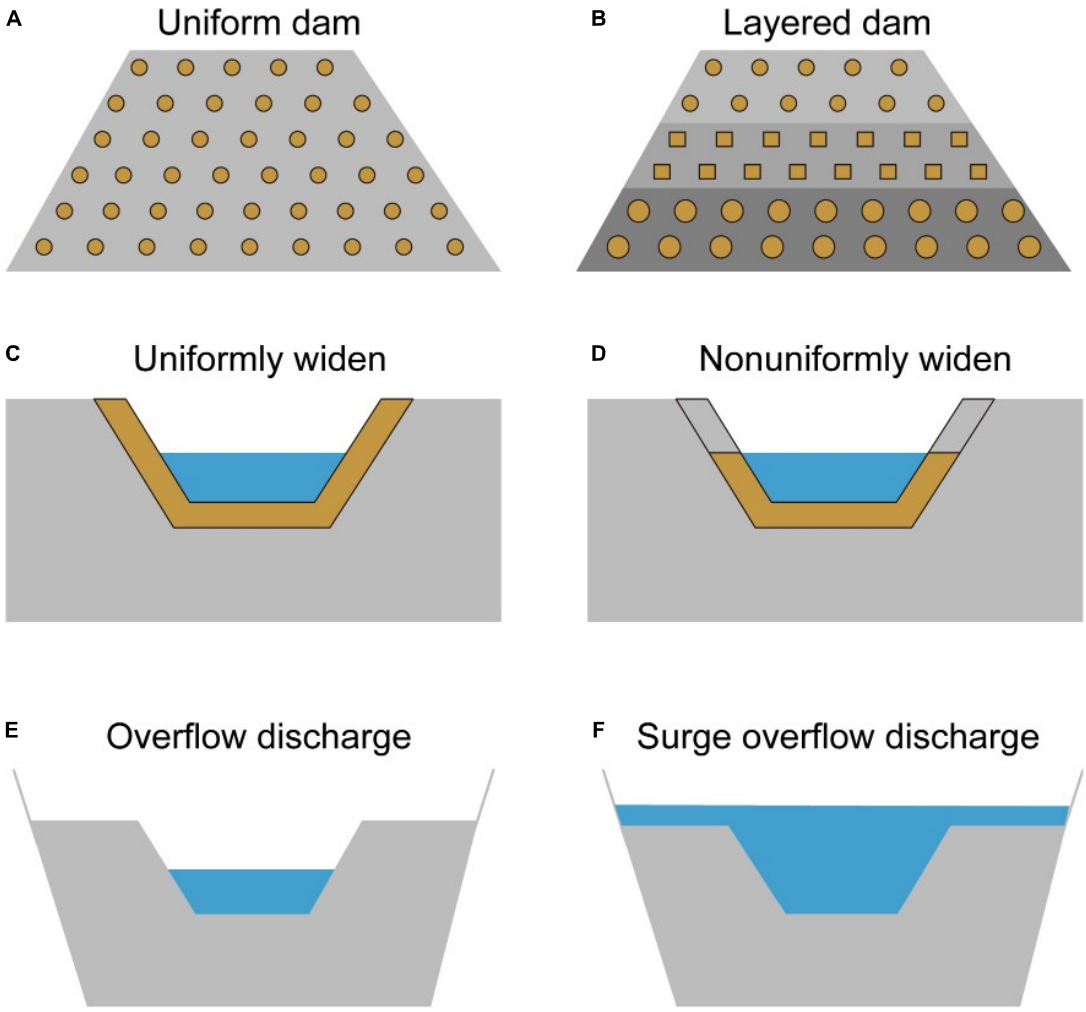

FIGURE 11 | Modifications of models of overtopping failure in a landslide dam: **(A,B)** uniform and layered distribution of dam materials, respectively (Chang and Zhang, 2010); **(C,D)** uniformly and non-uniformly widening the breach, respectively (Zhong et al., 2018); **(E)** outflow discharge within the breach; and **(F)** outside and within the breach (Wu and Li, 2017).

review will not introduce other computational fluid dynamics methods in detail.

Unfortunately, the overtopping failure predictions of landslide dams contain some uncertainty (Coleman et al., 2002; Zhu et al., 2004). The overtopping failure process of a landslide dam is believed to depend on the various factors introduced in Section "Influences of Characteristic Parameters on Landslide Dam Stability," including the landslide triggers, geomorphic characteristics, and dam materials. These factors vary greatly from case to case. At present, the numerical models of overtopping failures in landslide dams have some disadvantages. After a landslide dam has formed, it is difficult to rapidly obtain the soil parameters of the dam. Almost all of the simulations available are limited to overtopping failures in homogeneous dams, which is not consistent with the heterogeneity of landslide dams. In addition, the coupled erosion rate equations in the shallow water hydrodynamic models are empirical, and the entrainment parameters need to be calibrated for every landslide dam case. Furthermore, the capacity of the breaching flood to transport sediment has not been included in most modeling.

SEEPAGE FAILURE ANALYSES OF LANDSLIDE DAMS

Piping and flowing soil are typical phenomena of seepage failure in landslide dams. Laboratory tests and numerical simulations are the main research approaches to investigate the seepage failure of landslide dams.

Experimental Analyses of Seepage Failure

The experimental research investigating the seepage failure of landslide dams could be categorized into element and model tests. The element tests of seepage failure are also known as permeability tests, and the specimen sizes used in these tests are

small. Model tests carried out with appropriate proportions and similar materials resemble prototype testing.

Element Tests of Seepage Failure

The failure process of piping and flowing soil could be observed in various experiments. Based on the pore pressures in sandy soils, four stages of piping development were identified: initial movement, progressive heave, boil formation, and total heave (Fleshman and Rice, 2013, 2014). For widely graded material, the finer fraction in the initial stage moves as uniform loss across the entire base and a distinctly preferential path (piping) develops in the last stage (Moffat et al., 2011; Huang et al., 2015). Influenced by the amount and types of fine particles present in the non-cohesive and cohesive soils, three modes of piping behaviors were recognized: concentrated leak erosion, backward erosion, and suffusion (Richards and Reddy, 2012). The flowing soil failure of uniform sand is associated with an effective stress equal to zero, whereas a piping failure is caused by the internal erosion of fine particles in gap-graded sand (Ke and Takahashi, 2014; Van Beek et al., 2014; Yang and Wang, 2017).

The permeability coefficient and critical hydraulic gradient could be obtained from an element test to evaluate seepage stability (Richards and Reddy, 2007; Fleshman and Rice, 2013; Zhou et al., 2016; Zhu et al., 2019). The critical hydraulic gradient for seepage failure caused by flowing soil may be consistent with Terzaghi's theoretical value (Fontana, 2008; Huang et al., 2015; Yang and Wang, 2017). However, the critical hydraulic gradient for seepage failure caused by piping erosion is smaller than Terzaghi's theoretical value.

Based on grain size measures such as d_{15}, d_{85}, and grain sizes ranging from d to $4d$, the Kezdi (1979), Sherard (1979), and Kenney and Lau (1986) criteria have been proposed to ascertain the seepage stability. These geometric criteria were verified and modified by subsequent researchers (Burenkova, 1993; Skempton and Brogan, 1994; Richards and Reddy, 2007; Li and Fannin, 2008; Wan and Fell, 2008; Shire et al., 2014; Zhou et al., 2016). Considering the high coarse fraction in the landslide dam materials, Chang and Zhang (2013) extended the internal stability criteria for gap-graded and well-graded soils based on a physical understanding of the microstructures of the soils.

Grain compositions of landslide dams differ significantly between various landslide dams or even for a specific dam, resulting in different seepage failures. Shi et al. (2018) conducted seepage tests on four typical dam materials: fine-grained, coarse-grained, well-graded, and gap-graded materials at various dry densities, based on Tangjiashan landslide dam (Chang et al., 2011; Zhao et al., 2013). The seepage failures of the fine-grained and gap-graded soils were flowing soil (Shi et al., 2018). By contrast, they were piping for the coarse-grained and well-graded soils.

Model Tests of Seepage Failure

The prediction index of seepage failure of landslide dams is discerned in various experiments. The critical hydraulic gradients corresponding to the onset of seepage erosion and collapse of the dam crest were found to increase with an increase in the uniformity coefficient of dam material (Okeke and Wang, 2016a). The potential to form a piping path through the dams is reduced with an increase in the soil density and the homogeneity of the dam materials (Okeke and Wang, 2016b). The premonitory factors during the seepage failure were identified by Wang et al. (2018) as self-potential change, pore-pressure change, and seepage-water turbidity.

The seepage failure of landslide dams can be classified into four patterns based on the dam materials as shown in **Figure 12**. For a fine-grained landslide dam, the crest width is shortened by the slide of the downstream slope, and then the sliding area on the downstream side increasingly expands to the entire downstream slope: a typical sliding failure (Wang et al., 2018; Jiang et al., 2019; Zhu et al., 2019). This failure pattern is a combination of a flowing soil failure and an overtopping failure. For a coarse-grained landslide dam, the inflow rate and seepage flow rate basically maintain a balance and dam failure is not observed (Guan, 2018). For a well-graded landslide dam, the flow erodes the crest and downstream surface after the water level rises above the crest: a typical erosion failure (Xiong et al., 2018). This failure pattern is a combination of internal erosion and overtopping failures. Step-pool systems develop during the failure process, which is consistent with observations of the Tiger-leaping Gorge and Yujunmen landslide dams (Wang et al., 2009, 2012). For a gap-graded landslide dam, some fine grains are removed from the cracks driven by hydraulic gradient and these cracks easily broaden and interconnect, which eventually contributes to the formation of the piping channel: a typical piping failure (Xiong et al., 2018). This failure pattern was applicable to the landslide dam in the La Paz river catchment (Quenta et al., 2007).

Numerical Analyses of Seepage Failure

Compared with element and model tests, numerical analyses of seepage failure can provide a great deal of insight into the seepage process and hence the failure mechanisms of landslide dams. Currently, continuous medium methods and discontinuous medium methods are employed to analyze the seepage stability of landslide dams.

Continuous Medium Method

The finite-element method (FEM) and finite-difference method (FDM) are typical continuous medium methods. The distributions of the seepage field, stress, and displacement can be obtained using these methods, and the tendency of seepage failure is then determined as shown in **Figure 13**.

Considering the detachment of the soil grains from the soil fabric, backward erosion and the development of the piping path are presented as they vary with the grain compositions, porosity, and pore pressure (Fujisawa et al., 2010). The critical hydraulic gradient and the progression of internal erosion could be obtained by capturing the main hydraulic characteristics of the turbulent flow that occur in an erodible pipe and the seepage flow in the remaining area of a dam foundation (Wang et al., 2014; Rotunno et al., 2019). The heterogeneity could accelerate the development of preferential flow paths and increase the likelihood of seepage failures by verifying the stochastic parameters of the dam material, such as the hydraulic conductivity, void ratio, and grain contents (Liang et al., 2017). A local critical gradient rather than an average critical gradient

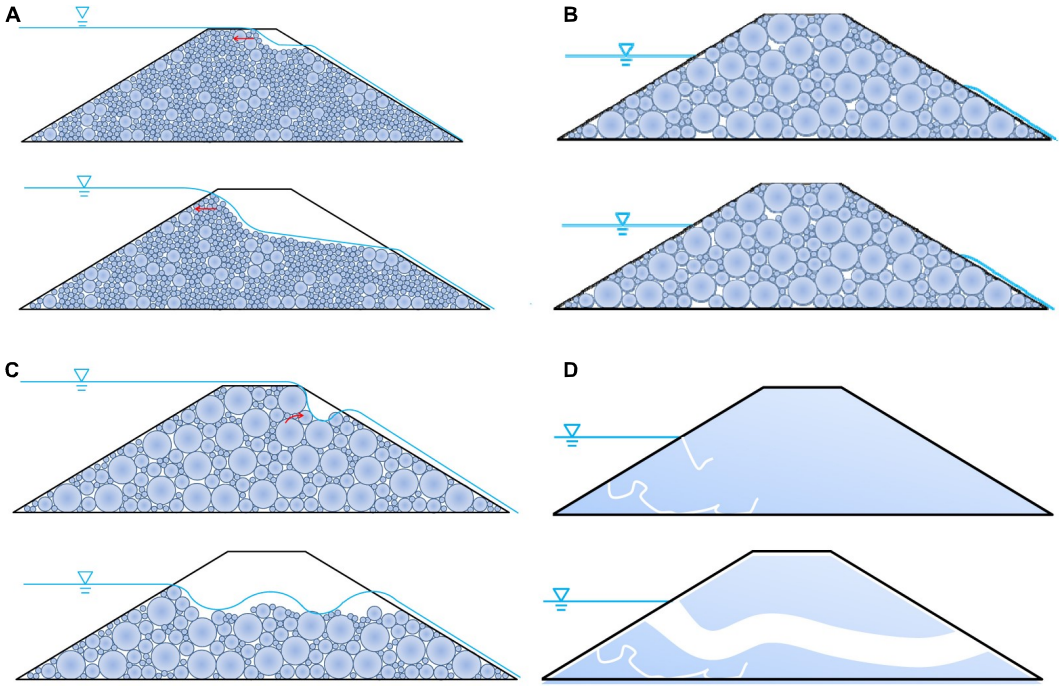

FIGURE 12 | Failure patterns of a landslide dam for different materials: **(A)** sliding failure for a fine-grained landslide dam (Wang et al., 2018; Jiang et al., 2019; Zhu et al., 2019); **(B)** no failure for a coarse-grained landslide dam; **(C)** erosion failure for a well-graded landslide dam (Xiong et al., 2018); **(D)** piping failure for a gap-graded landslide dam (Quenta et al., 2007; Xiong et al., 2018).

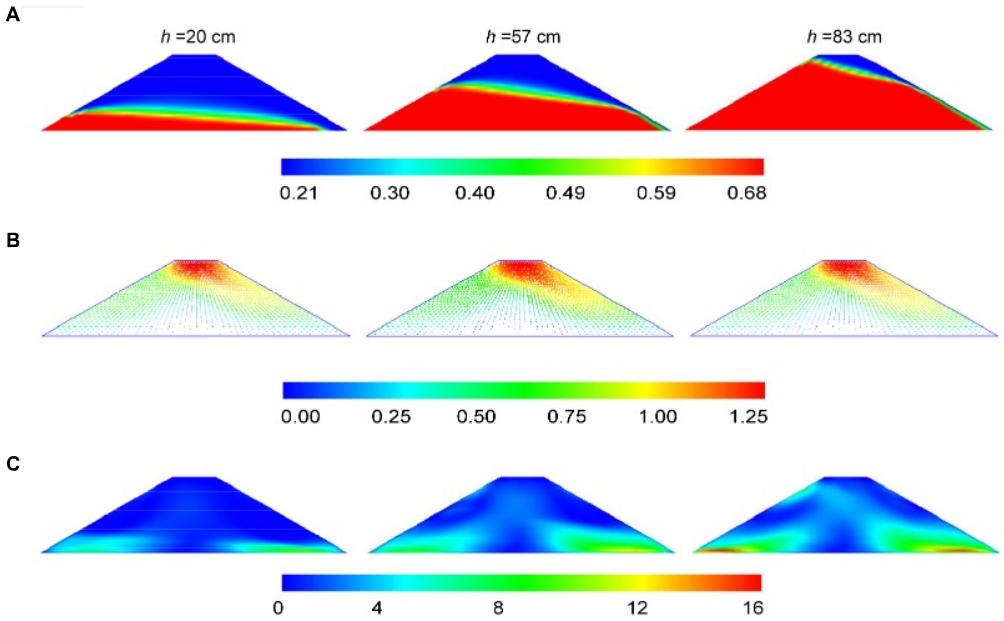

FIGURE 13 | Evolution of **(A)** saturation degree, **(B)** displacement field, and **(C)** shear strain during a seepage failure process (Xiong et al., 2018).

should be used as the criterion for pipe progression to account for the scale effects observed between large- and small-scale experiments (Robbins, 2016). Based on a rational constitutive model for a saturated/unsaturated soil (Zhang and Ikariya, 2011), Xiong et al. (2018) correlated fine-grained, well-graded, and gap-graded dam materials with the sliding failure, erosion failure, and piping failure by analyzing the development of the seepage lines, displacement field, saturation degree, and shear strain.

Discontinuous Medium Method

Compared with the continuous medium method, the discontinuous medium method has the outstanding advantage of simulating the interactions among particles. The discrete-element method (DEM) is a typical method based on the discontinuous media theory.

The process of internal erosion in landslide dams could be simulated by progressively removing the finer particles, and the mechanical consequences of erosion can thus be analyzed. The removal of particles produces an increase in the specific volume because of the solid volume decrease and void volume increase. The removal of fine grains leads to a decrease of the sliding resistance of each interparticle contact and the occurrence of local sliding, which contributes to the instability of the granular assemblies at a shear stress level much lower than the critical state failure line (Muir et al., 2010; Hicher, 2013). The number of contacts between the fine particles is significantly reduced by the fine particle loss, while the contact forces gradually transfer to the coarse soil particles (Zhang et al., 2019).

Alternatively, the migration process of the soil particles moved by the pore fluid could be directly simulated by coupling DEM with computational fluid dynamics (Zheng et al., 2018; Zhang et al., 2020). The representative size ratio of the soil skeleton has a great influence on the effectiveness of preventing the dam soil from being eroded (Huang Q.F. et al., 2014). The eroded percentage of soil particles gradually grows with the increase of the representative size ratio of the soil skeleton, and the effective vertical stresses reach zero when the hydraulic gradient reaches the estimated critical hydraulic gradient (Abdelhamid and El Shamy, 2015; Wang W. et al., 2017). The internal erosion rate is proportional to the flow velocity for both spherical and non-spherical particles, and a critical velocity exists for angular particles owing to grain interlocking which is not observed for the spherical particles (Guo et al., 2018). As shown in **Figure 14**, the seepage field is distributed uniformly in the fine-grained dam material which results in a global seepage failure (flowing soil), whereas it is gradually deflected with the increase in the hydraulic gradient and local seepage failure (piping) occurs in the coarse-grained dam material (Cheng et al., 2018; Shi et al., 2018).

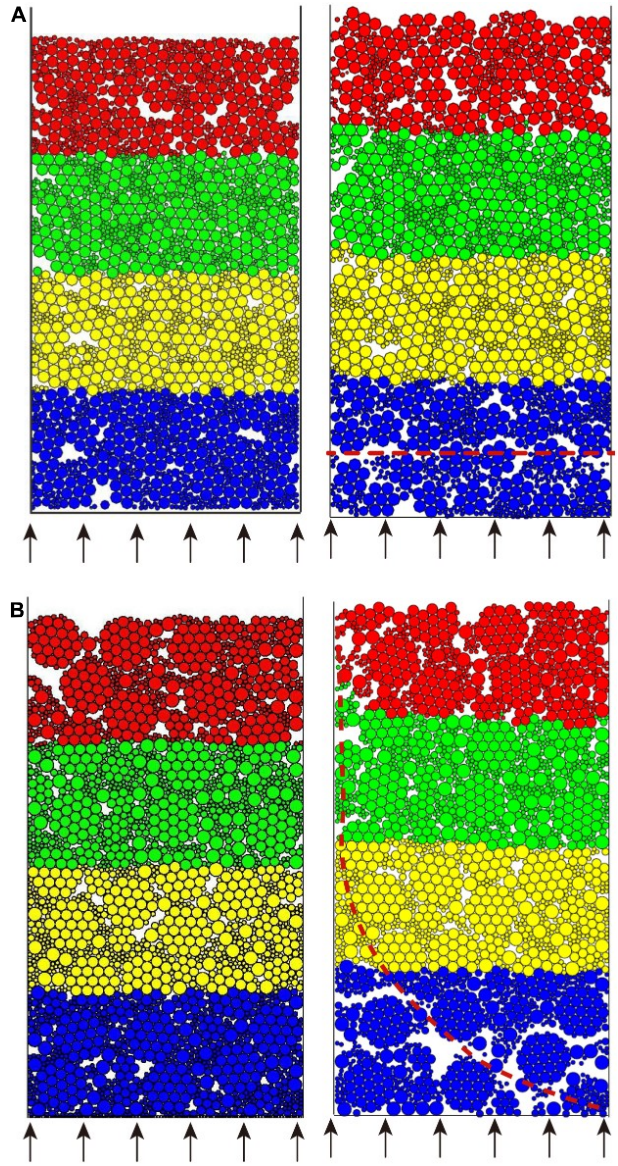

FIGURE 14 | Seepage failure modes in **(A)** fine-grained and **(B)** coarse-grained soils (Shi et al., 2018). The red dashed lines denote the seepage failure tendency. Flowing soil and piping failures occur for the fine-grained and coarse-grained soils, respectively.

FUTURE RESEARCH DIRECTIONS

The research on landslide dam stability is of enormous significance for early warnings and emergency evacuations and, consequently, also for disaster mitigation after dam failure. Considerable progress has been made over more than 30 years in characteristic analysis and developing some understanding of the failure mechanisms. Nevertheless, a complete understanding of the stability evaluation and failure mechanisms of a landslide dam remain elusive, and the state-of-the-art in failure modeling is far from advanced. The suggestions are listed as follows:

(1) The erosion rate of dam materials should be taken into account in the multifactor evaluation of the stability of a landslide dam. The erosion rate of dam materials can be obtained by *in situ* tests (i.e., Chang and Zhang, 2010; Chang et al., 2011) and laboratory model tests. However, most landslide dams last a short time, mainly because of the high erosion rate (Chang et al., 2011). It is necessary to establish the functional relationship between the grain composition and erosion rate by laboratory model tests to achieve the goal of rapid assessment. A similar approach is that the internal erosion of dam materials caused by seepage can be evaluated from the grain composition, like the Sherard (1979) and Kenney and Lau (1986) criteria. Moreover, the erosion function of the dam materials could be embedded in physically-based models and coupled

shallow water hydrodynamic models. The overtopping failure process of a landslide dam could then be rapidly predicted with high accuracy.

(2) The morphological characteristics of a landslide dam can be rapidly obtained by remote sensing or unmanned aerial vehicle (UAV). However, the grain composition and material distribution are difficult to determine. Traditionally, the grain size distribution of a landslide dam is obtained by sieve analysis. However, sieve analyses are impractical when dealing with materials often ranging in size from blocks tens of cubic meters in size to microscopic particles. The sampling method of grid by number analysis has been proposed to obtain the coarser part of the debris material (Casagli et al., 2003). Considering landslide dams located in remote mountainous areas, hyperspectral remote sensing technology is suggested to obtain the grain size on the surface of landslide dams. The hyperspectral system is now able to cover the wavelength region from 0.4 to 2.5 μm using hundreds of spectral channels (Li et al., 2012). The grain size can be determined by the hyperspectral technology in tandem with machine learning methods.

(3) Many research studies have been conducted for single landslide dams, investigating the breach discharge and failure pattern (Coleman et al., 2002; Schmocker and Hager, 2009; Walder et al., 2015; Jiang et al., 2016; Zhou G.G.D. et al., 2019). The outburst flood released by a landslide dam upstream can induce failures of downstream landslide dams one after another (Shi et al., 2015a). The breach of cascading landslide dams may result in a sharp increase in the peak outflow rate and thus a more serious disaster downstream. These research results of single landslide dams may not be suitable for cascading landslide dams due to the complex breach process and unsteady inflow rate (Shi et al., 2015a). In addition, the research attention paid to the cascading failure of landslide dams has been relatively limited. The effects of grain composition and geomorphic characteristics (dam geometry and initial water level) of landslide dams upstream and downstream on the cascading failure process and the amplification effect of breach discharge have not been explored.

(4) Significant differences in grain compositions occur in various dam zones because of grain segregation in the landslide dam accumulation process (Zhou Y.Y. et al., 2019). The grain composition near the bank may be different from that away from the bank. It is also applicable to the grain compositions in the dam upstream and downstream. The failure process and pattern caused by overtopping and seepage could be affected by this heterogeneity. However, the model dam is normally prepared manually by uniformly mixing the debris material. A sectionalized dam model should be considered in the corresponding model experiments and numerical analyses.

(5) The evolution of the flow properties during an overtopping failure should be considered in the corresponding model experiments and numerical analyses. The released flow changes from a pure water flow into a sediment flow or even a debris flow by substantial entrainment of dam materials (Chen et al., 2004; Zhou G.G.D. et al., 2019). The flow density and viscosity increase during the breach process which affects the erosion potential of dam material. Despite the importance of this, the enlargement process of debris flows during an overtopping failure is relatively unexplored (Chen et al., 2014; Chen H.Y. et al., 2015; Jiang et al., 2016; Zheng et al., 2016). In addition, the capacity of the overflow to transport sediment should be considered in the modeling.

(6) The effects of seepage on the overtopping failure of landslide dams should be investigated. At present, the overtopping and seepage failures are separately analyzed. Actually, seepage has a significant effect on the breach process and breach mode during overtopping. On the one hand, significant positive pore pressure occurs in the dam below seepage line and reduces the effective stress in the downstream slope. The pore pressures display an obvious difference among various dam materials and thus affect the overtopping failure (Peng et al., 2019). On the other hand, negative pore pressure is generated in the finer material with the apparent cohesion above the seepage line (Pickert et al., 2011). However, it is difficult to observe in the coarse-grained material. Coarser grains with a higher strength lead to a faster breach process compared with finer materials with a smaller strength (Morris et al., 2007; Zhong et al., 2019). This seemingly contradictory conclusion is closely related with pore pressure.

AUTHOR CONTRIBUTIONS

HZ and ZS finished the manuscript. DS and CM collected the data and landslide dam cases. MP, KH, and LZ modified the manuscript. All authors contributed to the article and approved the submitted version.

FUNDING

The research reported in this manuscript was substantially supported by the Natural Science Foundation of China (Nos. 42007252 and 41731283).

ACKNOWLEDGMENTS

The authors thank Mingzi Jiang for their help to collect the landslide dam cases.

SUPPLEMENTARY MATERIAL

The Supplementary Material for this article can be found online at: https://www.frontiersin.org/articles/10.3389/feart.2021.659935/full#supplementary-material

REFERENCES

Abdelhamid, Y., and El Shamy, U. (2015). Pore-scale modeling of fine-particle migration in granular filters. *Int. J. Geomech.* 16:04015086. doi: 10.1061/(asce)gm.1943-5622.0000592

Acharya, T. D., Mainali, S. C., Yang, I. T., and Lee, D. H. (2016). "Analysis of Jure landslide dam, Sindhupalchowk using GIS and remote sensing," in *The International Archives of Photogrammetry, Remote Sensing and Spatial Information Sciences*, Vol. 41, Prague, 201. doi: 10.5194/isprsarchives-xli-b6-201-2016

Arabshahi, H., and Lotfi, V. (2008). Earthquake response of concrete gravity dams including dam-foundation interface nonlinearities. *Eng. Struct.* 30, 3065–3073. doi: 10.1016/j.engstruct.2008.04.018

Bilici, Y., Bayraktar, A., Soyluk, K., Haciefendioğlu, K., Ates, S., and Adanur, S. (2009). Stochastic dynamic response of dam–reservoir–foundation systems to spatially varying earthquake ground motions. *Soil Dyn. Earthq. Eng.* 29, 444–458. doi: 10.1016/j.soildyn.2008.05.001

Bonnard, C. (2004). "Technical and human aspects of historic rockslide dammed lakes and landslide dam breaches," in *Security of Natural and Artificial Rockslide Dams, Extended Abstracts Volume, NATO Advanced Research Workshop*, eds K. Abdrakhmatov, S. G. Evans, R. Hermanns, G. Scarascia-Mugnozza, and A. L. Strom (Bishkek), 13–19.

Burenkova, V. V. (1993). "Assessment of suffusion in non-cohesive and graded soils," in *Proceedings of Filters in Geotechnical and Hydraulic Engineering*, Karlsruhe, 357–360.

Calayir, Y., and Karaton, M. (2005). A continuum damage concrete model for earthquake analysis of concrete gravity dam–reservoir systems. *Soil Dyn. Earthq. Eng.* 25, 857–869. doi: 10.1016/j.soildyn.2005.05.003

Canuti, P., Casagli, N., and Ermini, L. (1998). "Inventory of landslide dams in the Northern Apennine as a model for induced flood hazard forecasting," in *Managing Hydro-Geological Disasters in a Vulnerable Environment*, Perugia: CNR-GNDCI and UNESCO IHP, 189–202.

Cao, Z., Yue, Z., and Pender, G. (2011a). Flood hydraulics due to cascade landslide dam failure. *J. Flood Risk Manag.* 4, 104–114. doi: 10.1111/j.1753-318x.2011.01098.x

Cao, Z., Yue, Z., and Pender, G. (2011b). Landslide dam failure and flood hydraulics. Part I: experimental investigation. *Nat. Hazards* 59, 1003–1019. doi: 10.1007/s11069-011-9814-8

Cao, Z., Yue, Z., and Pender, G. (2011c). Landslide dam failure and flood hydraulics. Part II: coupled mathematical modelling. *Nat. Hazards* 59, 1021–1045. doi: 10.1007/s11069-011-9815-7

Capra, L. (2006). Abrupt climatic changes as triggering mechanisms of massive volcanic collapses. *J. Volcanol. Geotherm. Res.* 155, 329–333. doi: 10.1016/j.jvolgeores.2006.04.009

Casagli, N., and Ermini, L. (1999). Geomorphic analysis of landslide dams in the Northern Apennine. *Trans. Jpn. Geomorphol. Union* 20, 219–249.

Casagli, N., Ermini, L., and Rosati, G. (2003). Determining grain size distribution of the material composing landslide dams in the Northern Apennine: sampling and processing methods. *Eng. Geol.* 69, 83–97. doi: 10.1016/s0013-7952(02)00249-1

Chang, D. S., and Zhang, L. M. (2010). Simulation of the erosion process of landslide dams due to overtopping considering variations in soil erodibility along depth. *Nat. Hazards Earth Syst. Sci.* 10, 933–946. doi: 10.5194/nhess-10-933-2010

Chang, D. S., and Zhang, L. M. (2013). Extended internal stability criteria for soils under seepage. *Soils Found.* 53, 569–583. doi: 10.1016/j.sandf.2013.06.008

Chang, D. S., Zhang, L. M., Xu, Y., and Huang, R. Q. (2011). Field testing of erodibility of two landslide dams triggered by the 12 May Wenchuan earthquake. *Landslides* 8, 321–332. doi: 10.1007/s10346-011-0256-x

Chen, C. Y., and Chang, J. M. (2016). Landslide dam formation susceptibility analysis based on geomorphic features. *Landslides* 13, 1019–1033. doi: 10.1007/s10346-015-0671-5

Chen, C. Y., Chen, T. C., Yu, F. C., and Hung, F. Y. (2004). A landslide dam breach induced debris flow–a case study on downstream hazard areas delineation. *Eng. Geol.* 47, 91–101. doi: 10.1007/s00254-004-1137-6

Chen, H. Y., Cui, P., and Chen, X. Q. (2015). Laboratory experiments of water pressure loads acting on a downstream dam caused by ice avalanches. *Landslides* 12, 1131–1138. doi: 10.1007/s10346-014-0532-7

Chen, H. Y., Cui, P., Zhou, G. G. D., Zhu, X. H., and Tang, J. B. (2014). Experimental study of debris flow caused by domino failures of landslide dams. *Int. J. Sediment Res.* 29, 414–422. doi: 10.1016/s1001-6279(14)60055-x

Chen, M. T., and Harichandran, R. S. (2001). Response of an earth dam to spatially varying earthquake ground motion. *J. Eng. Mech.* 127, 932–939. doi: 10.1061/(asce)0733-9399(2001)127:9(932)

Chen, R., Shao, S., and Liu, X. (2015). Water–sediment flow modeling for field case studies in Southwest China. *Nat. Hazards* 78, 1197–1224. doi: 10.1007/s11069-015-1765-z

Chen, S. C., Lin, T. W., and Chen, C. Y. (2015). Modeling of natural dam failure modes and downstream riverbed morphological changes with different dam materials in a flume test. *Eng. Geol.* 188, 148–158. doi: 10.1016/j.enggeo.2015.01.016

Chen, S. S., Huo, J. P., and Zhang, W. M. (2008). Analysis of effects of "5.12" Wenchuan Earthquake on Zipingpu Concrete Face Rock-fill Dam. *Chin. J. Geotech. Eng.* 30, 795–801.

Chen, X., Cui, P., You, Y., Cheng, Z. L., Khan, A., Ye, C. Y., et al. (2017). Dam-break risk analysis of the Attabad landslide dam in Pakistan and emergency countermeasures. *Landslides* 14, 675–683. doi: 10.1007/s10346-016-0721-7

Chen, X. Q., Zhao, W. Y., Gao, Q., Jia, S. T., and Zhu, X. H. (2011). Experimental research on effect of man-made structure controlling dam-break flood. *Chin. J. Mount. Sci.* 29, 217–225.

Chen, Z. Y., Ma, L. Q., Yu, S., Chen, S. J., Zhou, X. B., Sun, P., et al. (2015). Back analysis of the draining process of the Tangjiashan barrier lake. *J. Hydraul. Eng.* 141:05014011. doi: 10.1061/(asce)hy.1943-7900.0000965

Cheng, K., Wang, Y., and Yang, Q. (2018). A semi-resolved CFD-DEM model for seepage-induced fine particle migration in gap-graded soils. *Comput. Geotech.* 100, 30–51. doi: 10.1016/j.compgeo.2018.04.004

Chigira, M., Wu, X., Inokuchi, T., and Wang, G. (2010). Landslides induced by the 2008 Wenchuan earthquake. Sichuan, China. *Geomorphology* 118, 225–238. doi: 10.1016/j.geomorph.2010.01.003

Coleman, S. E., Andrews, D. P., and Webby, M. G. (2002). Overtopping breaching of noncohesive homogeneous embankments. *J. Hydraul. Eng.* 128, 829–838. doi: 10.1061/(asce)0733-9429(2002)128:9(829)

Costa, J. E., and Schuster, R. L. (1988). The formation and failure of natural dams. *Geol. Soc. Am. Bull.* 100, 1054–1068. doi: 10.1130/0016-7606(1988)100<1054:tfafon>2.3.co;2

Costa, J. E., and Schuster, R. L. (1991). *Documented Historical Landslide Dams From Around the World*. U.S. Geological Survey Open-File Report. Reston, VA: U.S. Geological Survey, 91–239.

Crosta, G. B., Chen, H., and Lee, C. F. (2004). Replay of the 1987 Val Pola Landslide. Italian Alps. *Geomorphology* 60, 127–146. doi: 10.1016/j.geomorph.2003.07.015

Cui, P., Dang, C., Zhuang, J. Q., You, Y., Chen, X. Q., and Scott, K. M. (2012). Landslide-dammed lake at Tangjiashan, Sichuan Province, China (triggered by the Wenchuan Earthquake, May 12, 2008): risk assessment, mitigation strategy, and lessons learned. *Environ. Earth Sci.* 65, 1055–1065. doi: 10.1007/s12665-010-0749-2

Cui, P., Zhou, G. G. D., Zhu, X. H., and Zhang, J. Q. (2013). Scale amplification of natural debris flows caused by cascading landslide dam failures. *Geomorphology* 182, 173–189. doi: 10.1016/j.geomorph.2012.11.009

Cui, P., Zhu, Y., Han, Y., Chen, X. Q., and Zhuang, J. Q. (2009). The 12 May Wenchuan earthquake-induced landslide lakes: distribution and preliminary risk evaluation. *Landslides* 6, 209–223. doi: 10.1007/s10346-009-0160-9

Dazzi, S., Vacondio, R., and Mignosa, P. (2019). Integration of a levee breach erosion model in a GPU-accelerated 2D shallow water equations code. *Water Resour. Res.* 55, 682–702. doi: 10.1029/2018wr023826

Do, X. K., Kim, M., Nguyen, H. P. T., and Jung, K. (2016). Analysis of landslide dam failure caused by overtopping. *Proc. Eng.* 154, 990–994. doi: 10.1016/j.proeng.2016.07.587

Dong, J. J., Lai, P. J., Chang, C. P., Yang, S. H., Yeh, K. C., Liao, J. J., et al. (2014). Deriving landslide dam geometry from remote sensing images for the rapid assessment of critical parameters related to dam-breach hazards. *Landslides* 11, 93–105. doi: 10.1007/s10346-012-0375-z

Dong, J. J., Li, Y. S., Kuo, C. Y., Sung, R. T., Li, M. H., Lee, C. T., et al. (2011).). The formation and breach of a short-lived landslide dam at Hsiaolin village, Taiwan-part I: post-event reconstruction of dam geometry. *Eng. Geol.* 123, 40–59. doi: 10.1016/j.enggeo.2011.04.001

Dong, J. J., Tung, Y. H., Chen, C. C., Liao, J. J., and Pan, Y. W. (2009). Discriminant analysis of the geomorphic characteristics and stability of landslide dams. *Geomorphology* 110, 162–171. doi: 10.1016/j.geomorph.2009.04.004

Ehteshami-Moinabadi, M., and Nasiri, S. (2019). Geometrical and structural setting of landslide dams of the Central Alborz: a link between earthquakes and landslide damming. *Bull. Eng. Geol. Environ.* 78, 69–88. doi: 10.1007/s10064-017-1021-8

Ermini, L., and Casagli, N. (2003). Prediction of the behaviour of landslide dams using a geomorphological dimensionless index. *Earth Surf. Process. Landf.* 28, 31–47. doi: 10.1002/esp.424

Evans, S. G., Hermanns, R. L., Strom, A., and Scarascia-Mugnozza, G. (2011). *Natural and Artificial Rockslide Dams*, Vol. 133. Berlin: Springer Science & Business Media.

Fan, X., Dufresne, A., Subramanian, S. S., Strom, A., Hermanns, R., Stefanelli, C. T., et al. (2020). The formation and impact of landslide dams–State of the art. *Earth Sci. Rev.* 203:103116. doi: 10.1016/j.earscirev.2020.103116

Fan, X., Huang, R., Westen, C. J. V., Xu, Q., Havenith, H. B., and Jetten, V. (2014). "A conceptual event-tree model for coseismic landslide dam hazard assessment," in *Landslide Science for a Safer Geoenvironment*, (Berlin: Springer), 605–608. doi: 10.1007/978-3-319-04996-0_93

Fan, X., Westen, C. J. V., Xu, Q., Gorum, T., and Dai, F. C. (2012). Analysis of landslide dams induced by the 2008 Wenchuan earthquake. *J. Asian Earth Sci.* 57, 25–37. doi: 10.1016/j.jseaes.2012.06.002

Fan, X., Xu, Q., Alonso-Rodriguez, A., Subramanian, S. S., Li, W. L., Zheng, G., et al. (2019). Successive landsliding and damming of the Jinsha River in eastern Tibet, China: prime investigation, early warning, and emergency response. *Landslides* 16, 1003–1020. doi: 10.1007/s10346-019-01159-x

Fleshman, M. S., and Rice, J. D. (2013). Constant gradient piping test apparatus for evaluation of critical hydraulic conditions for the initiation of piping. *Geotech. Test. J.* 36, 834–846.

Fleshman, M. S., and Rice, J. D. (2014). Laboratory modeling of the mechanisms of piping erosion initiation. *J. Geotech. Geoenviron. Eng.* 140:04014017. doi: 10.1061/(asce)gt.1943-5606.0001106

Fontana, N. (2008). Experimental analysis of heaving phenomena in sandy soils. *J. Hydraul. Eng.* 134, 794–799. doi: 10.1061/(asce)0733-9429(2008)134:6(794)

Foster, M., Fell, R., and Spannagle, M. (2000). The statistics of embankment dam failures and accidents. *Can. Geotech. J.* 37, 1000–1024. doi: 10.1139/t00-030

Fread, D. L. (1988). *BREACH, an Erosion Model for Earthen Dam Failures*. Washington, DC: NOAA.

Frey, H., Huggel, C., Chisolm, R. E., Baer, P., McArdell, B., Cochachin, A., et al. (2018). Multi-source glacial lake outburst flood hazard assessment and mapping for Huaraz. Cordillera Blanca, Peru. *Front. Earth Sci.* 6:210. doi: 10.3389/feart.2018.00210

Fujisawa, K., Kobayashi, A., and Aoyama, S. (2009). Theoretical description of embankment erosion owing to overflow. *Géotechnique* 59, 661–671. doi: 10.1680/geot.7.00035

Fujisawa, K., Murakami, A., and Nishimura, S. (2010). Numerical analysis of the erosion and the transport of fine particles within soils leading to the piping phenomenon. *Soils Found.* 50, 471–482. doi: 10.3208/sandf.50.471

Gariano, S. L., and Guzzetti, F. (2016). Landslides in a changing climate. *Earth Sci. Rev.* 162, 227–252. doi: 10.1016/j.earscirev.2016.08.011

Gregoretti, C., Maltauro, A., and Lanzoni, S. (2010). Laboratory experiments on the failure of coarse homogeneous sediment natural dams on a sloping bed. *J. Hydraul. Eng.* 136, 868–879. doi: 10.1061/(asce)hy.1943-7900.0000259

Guan, S. G. (2018). *Influence of Landslide Dam Materials on Dam Failure Modes and Interation Mechanism of Muti-Dam Cascading Breaching*. PhD thesis, Shanghai: Tongji University, 28–55.

Guo, Y., Yang, Y., and Yu, X. B. (2018). Influence of particle shape on the erodibility of non-cohesive soil: insights from coupled CFD–DEM simulations. *Particuology* 39, 12–24. doi: 10.1016/j.partic.2017.11.007

Hager, W. H., Fritz, H. M., and Minor, H. E. (2004). Near field characteristics of landslide generated impulse waves. *J. Waterw. Port Coast. Ocean Eng.* 130, 287–302. doi: 10.1061/(asce)0733-950x(2004)130:6(287)

Hanson, G. J., Cook, K. R., and Temple, D. M. (2002). "Research results of large-scale embankment overtopping breach tests, in: dam safety 2002," in *Proceedings of the Association of State Dam Safety Officials*, Tampa, FL. doi: 10.21608/erjm.2013.67430

Hegan, B. D., Johnson, J. D., and Stevens, C. (2001). "Landslide risk from the Hipaua Geothermal Area near Waihi Village at the southern end of Lake Taupo. Engineering in Hazardous Terrain," in *Proceedings of New Zealand Geotechnical Society Symposium*, Christchurch, 439–448.

Hermanns, R. L. (2013). "Landslide dam," in *Encyclopedia of Natural Hazards*, ed. P. Bobrowsky (Berlin: Springer), 602–606.

Hicher, P. Y. (2013). Modelling the impact of particle removal on granular material behavior. *Géotechnique* 63, 118–128. doi: 10.1680/geot.11.p.020

Hu, X. W., Lu, X. P., Huang, R. Q., Ren, X. M., Wang, X. R., and Liu, J. (2009). Analyses of river-blocking and breaking mode of "9·24" debris flow near Tangjiashan barrier dam. *J. Southwest Jiaotong Univ.* 44, 312–320.

Huang, D., Chen, J., Chen, L., and Wang, S. (2015). Experimental study of the mechanism of flowing soil for homogeneous cohesionless soil. *Chin. J. Rock Mech. Eng.* 34, 3424–3431.

Huang, Q. F., Zhan, M. L., Sheng, J. C., Luo, Y. L., and Su, B. Y. (2014). Investigation of fluid flow-induced particle migration in granular filters using a DEM-CFD method. *J. Hydrodyn* 26, 406–415. doi: 10.1016/s1001-6058(14)60046-9

Huang, R., and Fan, X. (2013). The landslide story. *Nat. Geosci.* 6, 325–326. doi: 10.1038/ngeo1806

Huang, W., Cao, Z., Carling, P., and Pender, G. (2014). Coupled 2D hydrodynamic and sediment transport modeling of megaflood due to glacier dam-break in Altai Mountains. Southern Siberia. *J Mt. Sci.* 11, 1442–1453. doi: 10.1007/s11629-014-3032-2

Javadi, N., and Mahdi, T. F. (2014). Experimental investigation into rockfill dam failure initiation by overtopping. *Nat. Hazards* 74, 623–637. doi: 10.1007/s11069-014-1201-9

Jiang, X., Cui, P., Chen, H., and Guo, Y. (2016). Formation conditions of outburst debris flow triggered by overtopped natural dam failure. *Landslides* 14, 821–831. doi: 10.1007/s10346-016-0751-1

Jiang, X., and Wei, Y. (2019). Natural dam breaching due to overtopping: effects of initial soil moisture. *Bull. Eng. Geol. Environ.* 78, 4821–4831. doi: 10.1007/s10064-018-01441-7

Jiang, X., Wei, Y., Wu, L., Hu, K. H., Zhu, Z. Y., Zou, Z. Y., et al. (2019). Laboratory experiments on failure characteristics of non-cohesive sediment natural dam in progressive failure mode. *Environ. Earth Sci.* 78:538.

Kakinuma, T., and Shimizu, Y. (2014). Large-scale experiment and numerical modeling of a riverine levee breach. *J. Hydraul. Eng.* 140:04014039. doi: 10.1061/(asce)hy.1943-7900.0000902

Ke, L., and Takahashi, A. (2014). Experimental investigations on suffusion characteristics and its mechanical consequences on saturated cohesionless soil. *Soils Found.* 54, 713–730. doi: 10.1016/j.sandf.2014.06.024

Kenney, T., and Lau, D. (1986). Internal stability of granular filters: reply. *Can. Geotech. J.* 23, 420–423. doi: 10.1139/t86-068

Kezdi, A. (1979). *Soil Physics: Selected Topics*. Amsterdam: Elsevier.

Koo, W., and Kim, M. H. (2008). Numerical modeling and analysis of waves induced by submerged and aerial/sub-aerial landslides. *KSCE J. Civ. Eng.* 12, 77–83. doi: 10.1007/s12205-008-0077-1

Korup, O. (2002). Recent research on landslide dams-a literature review with special attention to New Zealand. *Prog. Phys. Geogr.* 26, 206–235. doi: 10.1191/0309133302pp333ra

Korup, O. (2004). Geomorphometric characteristics of New Zealand landslide dams. *Eng. Geol.* 73, 13–35. doi: 10.1016/j.enggeo.2003.11.003

Korup, O. (2005). Geomorphic imprint of landslides on alpine river systems, southwest New Zealand. *Earth Surf. Process. Landf.* 30, 783–800. doi: 10.1002/esp.1171

Korup, O., and Tweed, F. (2007). Ice, moraine, and landslide dams in mountainous terrain. *Quat. Sci. Rev.* 26, 3406–3422. doi: 10.1016/j.quascirev.2007.10.012

Kumar, V., Gupta, V., Jamir, I., and Chattoraj, S. L. (2019). Evaluation of potential landslide damming: case study of Urni landslide, Kinnaur, Satluj valley, India. *Geosci. Front.* 10, 753–767. doi: 10.1016/j.gsf.2018.05.004

Kuo, Y. S., Tsang, Y. C., Chen, K. T., and Shieh, C. L. (2011). Analysis of landslide dam geometries. *J Mt. Sci.* 8, 544–550. doi: 10.1007/s11629-011-2128-1

Li, J., Cao, Z., Pender, G., and Liu, Q. Q. (2013). A double layer-averaged model for dam-break flows over mobile bed. *J. Hydraul. Res.* 51, 518–534. doi: 10.1080/00221686.2013.812047

Li, M., and Fannin, R. J. (2008). Comparison of two criteria for internal stability of granular soil. *Can. Geotech. J.* 45, 1303–1309. doi: 10.1139/t08-046

Li, M. H., Sung, R. T., Dong, J. J., Lee, C. T., and Chen, C. C. (2011). The formation and breaching of a short-lived landslide dam at Hsiaolin Village, Taiwan—Part II: simulation of debris flow with landslide dam breach. *Eng. Geol.* 123, 60–71. doi: 10.1016/j.enggeo.2011.05.002

Li, P. Y., Zhou, X. Y., Wu, Q. F., and Chen, Y. S. (2008). Comprehensive introduction to disaster relief and strengthening of earthquake-induced dammed lake. *J. Yangtze River Sci. Res. Inst.* 25, 52–57.

Li, Z., Yang, R., Dang, F., Du, P., Zhang, X., Tan, B., et al. (2012). "A review on the geological applications of hyperspectral remote sensing technology," in *2012 4th Workshop on Hyperspectral Image and Signal Processing (WHISPERS)*, Shanghai.

Liang, Y., Yeh, T. C. J., Wang, Y. L., Liu, M. W., Wang, J. J., and Hao, Y. H. (2017). Numerical simulation of backward erosion piping in heterogeneous fields. *Water Resour. Res.* 53, 3246–3261. doi: 10.1002/2017wr020425

Liao, H. W., and Lee, C. T. (2000). "Landslides triggered by the Chi-Chi earthquake," in *Proceedings of the 21st Asian Conference on Remote Sensing*, Vol. 1, Taipei, 383–388.

Liu, J., Zhou, X. C., Chen, W., and Hong, X. (2019). Breach discharge estimates and surface velocity measurements for an Earth dam failure process due to overtopping based on the LS-PIV method. *Arab. J. Sci. Eng.* 44, 329–339. doi: 10.1007/s13369-018-3310-3

Liu, N., Yang, Q. G., and Chen, Z. Y. (2016). *Hazard Mitigation for Barrier Lakes*. Changjiang: Publishing House, Wuhan, 240–266.

Liu, W., and He, S. (2018). Dynamic simulation of a mountain disaster chain: landslides, barrier lakes, and outburst floods. *Nat. Hazards* 90, 757–775. doi: 10.1007/s11069-017-3073-2

Loukola, E., and Huokuna, M. (1998). "A numerical erosion model for embankment dams failure and its use for risk assessment," in *Proceedings of "CADAM (Concerted Action on Dam Break Modelling)"*, Munich: Munich Meeting, 8–9.

Memarzadeh, R., Barani, G., and Ghaeini-Hessaroeyeh, M. (2018). Application of a weakly compressible smoothed particle hydrodynamics multi-phase model to non-cohesive embankment breaching due to flow overtopping. *Front. Struct. Civ. Eng.* 012:412–424. doi: 10.1007/s11709-017-0432-8

Moffat, R., Fannin, R. J., and Garner, S. J. (2011). Spatial and temporal progression of internal erosion in cohesionless soil. *Can. Geotech. J.* 48, 399–412. doi: 10.1139/t10-071

Mohamed, A. A. A., Samuels, P. G., Morris, M. W., and Ghataora, G. S. (2002). "Improving the accuracy of prediction of breach formation through embankment dams and flood embankments," in *Proceedings of the International Conference on Fluvial Hydraulics, Louvain-la-Neuve*, Belgium.

Morris, M. W., Hassan, M., and Vaskinn, K. A. (2007). Breach formation: field test and laboratory experiments. *J. Hydraul. Res.* 45, 9–17. doi: 10.1080/00221686.2007.9521828

Morris, M. W., Kortenhaus, A., and Visser, P. J. (2009). *Modelling Breach Initiation and Growth. FLOODsite Report T06-08-02*. Wallingford: FLOODsite. FLOODsite Project, HR.

Muir, W. D., Maeda, K., and Nukudani, E. (2010). Modelling mechanical consequences of erosion. *Géotechnique* 60, 447–457. doi: 10.1680/geot.2010.60.6.447

Nian, T., Wu, H., Chen, G., Zheng, D., Zhang, Y., and Li, D. (2018). Research progress on stability evaluation method and disaster chain effect of landslide dam. *Chin. J. Rock Mech. Eng.* 37, 1796–1812.

Niu, Z., Xu, W., Li, N., Xue, Y., and Chen, H. (2012). Experimental investigation of the failure of cascade landslide dams. *J. Hydrodyn.* 24, 430–441. doi: 10.1016/s1001-6058(11)60264-3

Okeke, A. C. U., and Wang, F. (2016a). Critical hydraulic gradients for seepage-induced failure of landslide dams. *Geoenviron. Disasters* 3:9.

Okeke, A. C. U., and Wang, F. (2016b). Hydromechanical constraints on piping failure of landslide dams: an experimental investigation. *Geoenviron. Disasters* 3:4.

Ouyang, C., He, S., and Xu, Q. (2014). MacCormack-TVD finite difference solution for dam break hydraulics over erodible sediment beds. *J. Hydraul. Eng.* 141:06014026. doi: 10.1061/(asce)hy.1943-7900.0000986

Peng, M., and Zhang, L. M. (2012). Breaching parameters of landslide dams. *Landslides* 9, 13–31. doi: 10.1007/s10346-011-0271-y

Peng, M., and Zhang, L. M. (2013). Dynamic decision making for dam-break emergency management–Part 1: theoretical framework. *Nat. Hazards Earth Syst. Sci.* 13, 425–437. doi: 10.5194/nhess-13-425-2013

Peng, M., Zhang, L. M., Chang, D. S., and Shi, Z. M. (2014). Engineering risk mitigation measures for the landslide dams induced by the 2008 Wenchuan earthquake. *Eng. Geol.* 180, 68–84. doi: 10.1016/j.enggeo.2014.03.016

Peng, M., Jiang, Q. L., Zhang, Q. Z., Hong, Y., Jiang, M. Z., Shi, Z. M., et al. (2019). Stability analysis of landslide dams under surge action based on large-scale flume experiments. *Eng. Geol.* 259:105191. doi: 10.1016/j.enggeo.2019.105191

Pickert, G., Weitbrecht, V., and Bieberstein, A. (2011). Breaching of overtopped river embankments controlled by apparent cohesion. *J. Hydraul. Res.* 49, 143–156. doi: 10.1080/00221686.2011.552468

Pirocchi, A. (1992). "Laghi di sbarramento per frana nelle Alpi: tipologia ed evoluzione," in *Proceedings I Convegno Nazionale dei Giovani Ricercatori in Geologia Applicata, Gargnano Ricerca Scientifica Ed Educazione Permanente*, Vol. 93 (Milan: University of Milan), 128–136.

Powledge, G. R., Ralston, D. C., Miller, P., Chen, Y. H., Clopper, P. E., and Temple, D. M. (1989). Mechanics of overflow erosion on embankments. II: hydraulic and design considerations. *J. Hydraul. Eng.* 115, 1056–1075. doi: 10.1061/(asce)0733-9429(1989)115:8(1056)

Proulx, J., Paultre, P., Rheault, J., and Robert, Y. (2001). An experimental investigation of water level effects on the dynamic behaviour of a large arch dam. *Earthq. Eng. Struct. Dyn.* 30, 1147–1166. doi: 10.1002/eqe.55

Quenta, G., Galaza, I., Teran, N., Hermanns, R. L., Cazas, A., and García, H. (2007). *Deslizamiento Traslacional y Represamiento en el valle de Allpacoma, Ciudad de La Paz, Bolivia. Movimientos en Masa en la Región Andina–Una Guía Para la Evaluación de Amenazas, Proyecto Multinacional Andino: Geociencias para las Comunidades Andinas, Servicio Nacional de Geología y Minería*. Santiago: Publicación Geológica Multinacional, 230–234.

Ran, Q., Tong, J., Shao, S., Fu, X., and Xu, Y. (2015). Incompressible SPH scour model for movable bed dam break flows. *Adv. Water Resour.* 82, 39–50. doi: 10.1016/j.advwatres.2015.04.009

Richards, K. S., and Reddy, K. R. (2007). Critical appraisal of piping phenomena in earth dams. *Bull. Eng. Geol. Environ.* 66, 381–402. doi: 10.1007/s10064-007-0095-0

Richards, K. S., and Reddy, K. R. (2012). Experimental investigation of initiation of backward erosion piping in soils. *Géotechnique* 62, 933–942. doi: 10.1680/geot.11.p.058

Risley, J. C., Walder, J. S., and Denlinger, R. P. (2006). Usoi Dam wave overtopping and flood routing in the Bartang and Panj Rivers, Tajikistan. *Nat. Hazards* 38, 375–390. doi: 10.1007/s11069-005-1923-9

Robbins, B. A. (2016). Numerical modeling of backward erosion piping. *Appl. Numer. Model. Geomech.* 2016, 551–558.

Rotunno, A. F., Callari, C., and Froiio, F. (2019). A finite element method for localized erosion in porous media with applications to backward piping in levees. *Int. J. Numer. Anal. Methods Geomech.* 43, 293–316. doi: 10.1002/nag.2864

Sattar, A., and Konagai, K. (2012). "Recent landslide damming events and their hazard mitigation strategies," in *Advances in Geotechnical Earthquake Engineering–Soil Liquefaction and Seismic Safety of Dams and Monuments*, ed. A. Moustafa (London: IntechOpen), 219–232.

Schmocker, L., Frank, P. J., and Hager, W. H. (2014). Overtopping dike-breach: Effect of grain size distribution. *J. Hydraul. Res.* 52, 559–564. doi: 10.1080/00221686.2013.878403

Schmocker, L., and Hager, W. H. (2009). Modelling dike breaching due to overtopping. *J. Hydraul. Res.* 47, 585–597. doi: 10.3826/jhr.2009.3586

Schuster, R. L. (2000). "Outburst debris-flows from failure of natural dams," in *Proceedings 2nd International Conference on Debris Flow Hazard Mitigation*, Taipei, 16–20.

Schuster, R. L., and Alford, D. (2004). Usoi landslide dam and Lake Sarez, Pamir mountains, Tajikistan. *Environ. Eng. Geosci.* 10, 151–168. doi: 10.2113/10.2.151

Schuster, R. L., and Evans, S. G. (2011). "Engineering measures for the hazard reduction of landslide dams," in *Natural and Artificial Rockslide Dams, Lecture Notes in Earth Sciences*, eds S. G. Evans, R. L. Hermanns, A. Strom, and G. Scarascia-Mugnozza (Berlin: Springer), 77–100. doi: 10.1007/978-3-642-04764-0_2

Sevim, B., Altunişik, A. C., and Bayraktar, A. (2011). Earthquake behavior of Berke arch dam using ambient vibration test results. *J. Perform. Constr. Facil.* 26, 780–792. doi: 10.1061/(asce)cf.1943-5509.0000264

Shang, Y., Yang, Z., Li, L., Liu, D., Liao, Q., and Wang, Y. (2003). A super-large landslide in Tibet in 2000: background, occurrence, disaster, and origin. *Geomorphology* 54, 225–243. doi: 10.1016/s0169-555x(02)00358-6

Shen, D., Shi, Z., Peng, M., Zhang, L. M., and Jiang, M. Z. (2020). Longevity analysis of landslide dams. *Landslides* 17, 1797–1821. doi: 10.1007/s10346-020-01386-7

Shen, W. H., Liu, B. Y., and Shi, B. P. (2013). Triggering mechanism of aftershocks triggered by Wenchuan Mw 7.9 earthquake. *Acta Seismol. Sin.* 35, 461–476.

Sherard, J. L. (1979). "Sinkholes in dams of coarse, broadly graded soils," in *Proceeding of the 13th International Congress on Large Dams*, Vol. 2, New Delhi,, 25–35.

Shi, Z. M., Guan, S. G., Peng, M., Zhang, L. M., Zhu, Y., and Cai, Q. P. (2015a). Cascading breaching of the Tangjiashan landslide dam and two smaller downstream landslide dams. *Eng. Geol.* 193, 445–458. doi: 10.1016/j.enggeo.2015.05.021

Shi, Z. M., Wang, Y. Q., Peng, M., Chen, J. F., and Yuan, J. (2015b). Characteristics of the landslide dams induced by the 2008 Wenchuan earthquake and dynamic behavior analysis using large-scale shaking table tests. *Eng. Geol.* 194, 25–37. doi: 10.1016/j.enggeo.2014.10.009

Shi, Z. M., Wang, Y. Q., Peng, M., Guan, S. G., and Chen, J. F. (2015c). Landslide dam deformation analysis under aftershocks using large-scale shaking table tests measured by videogrammetric technique. *Eng. Geol.* 186, 68–78. doi: 10.1016/j.enggeo.2014.09.008

Shi, Z. M., Ma, X. L., Peng, M., and Zhang, L. M. (2014). Statistical analysis and efficient dam burst modelling of landslide dams based on a large-scale database. *Chin. J. Rock Mech. Eng.* 33, 1780–1790.

Shi, Z. M., Xiong, X., Peng, M., Zhang, L. M., Xiong, Y. F., Chen, H. X., et al. (2017). Risk assessment and mitigation for the Hongshiyan landslide dam triggered by the 2014 Ludian earthquake in Yunnan. China. *Landslides* 14, 269–285. doi: 10.1007/s10346-016-0699-1

Shi, Z. M., Zheng, H. C., Yu, S. B., and Peng, M. (2018). Application of CFD-DEM to investigate seepage characteristics of landslide dam materials. *Comput. Geotech.* 101, 23–33. doi: 10.1016/j.compgeo.2018.04.020

Shire, T., O'Sullivan, C., Hanley, K. J., and Fannin, R. J. (2014). Fabric and effective stress distribution in internally unstable soils. *J. Geotech. Geoenviron. Eng.* 140:04014072. doi: 10.1061/(asce)gt.1943-5606.0001184

Singh, V. P., and Scarlatos, P. D. (1988). Analysis of gradual earth-dam failure. *J. Hydraul. Eng.* 114, 21–42. doi: 10.1061/(asce)0733-9429(1988)114:1(21)

Skempton, A. W., and Brogan, J. M. (1994). Experiments on piping in sandy gravels. *Géotechnique* 44, 449–460. doi: 10.1680/geot.1994.44.3.449

Stefanelli, C. T., Catani, F., and Casagli, N. (2015). Geomorphological investigations on landslide dams. *Geoenviron. Disasters* 2:21.

Stefanelli, C. T., Segoni, S., Casagli, N., and Catani, F. (2016). Geomorphic indexing of landslide dams evolution. *Eng. Geol.* 208, 1–10. doi: 10.1016/j.enggeo.2016.04.024

Strom, A. (2010). Landslide dams in Central Asia region. *J. Jp.n Landslide Soc.* 47, 309–324. doi: 10.3313/jls.47.309

Swaisgood, J. R. (2003). "Embankment dam deformations caused by earthquakes," in *Pacific Conference on Earthquake Engineering*, Conifer, CO, 014.

Swanson, F. J., Oyagi, N., and Tominaga, M. (1986). *Landslide Dams in Japan, Landslide Dams: Processes, Risk, and Mitigation*. Reston, VA: ASCE, 131–145.

Tang, C. J., and Lee, J. F. (1992). Landslide-generated waves in reservoirs. *Proc. Eng. Mech.* 5, 220–223.

Van Beek, V. M., Bezuijen, A., Sellmeijer, J. B., and Barends, F. B. J. (2014). Initiation of backward erosion piping in uniform sands. *Géotechnique* 64, 927–941. doi: 10.1680/geot.13.p.210

Volz, C., Frank, P. J., Vetsch, D. F., Hager, W. H., and Boes, R. M. (2017). Numerical embankment breach modelling including seepage flow effects. *J. Hydraul. Res.* 55, 480–490. doi: 10.1080/00221686.2016.1276104

Walder, J. S., Iverson, R. M., Godt, J. W., Logan, M., and Solovitz, S. A. (2015). Controls on the breach geometry and flood hydrograph during overtopping of noncohesive earthen dams. *Water Resour. Res.* 51, 6701–6724. doi: 10.1002/2014wr016620

Wan, C. F., and Fell, R. (2008). Assessing the potential of internal instability and suffusion in embankment dams and their foundations. *J. Geotech. Geoenviron. Eng.* 134, 401–407. doi: 10.1061/(asce)1090-0241(2008)134:3(401)

Wang, D. Y., Fu, X. D., Jie, Y. X., Dong, W. J., and Hu, D. (2014). Simulation of pipe progression in a levee foundation with coupled seepage and pipe flow domains. *Soils Found.* 54, 974–984. doi: 10.1016/j.sandf.2014.09.003

Wang, F. W., Dai, Z. L., Okeke, C. A. U., and Mitani, Y. (2018). Experimental study to identify premonitory factors of landslide dam failures. *Eng. Geol.* 232, 123–134. doi: 10.1016/j.enggeo.2017.11.020

Wang, H. B., Sassa, K., and Xu, W. Y. (2007). Analysis of a spatial distribution of landslides triggered by the 2004 Chuetsu earthquakes of Niigata Prefecture. Japan. *Nat. Hazards* 41:43. doi: 10.1007/s11069-006-9009-x

Wang, M. (2018). *Numerical and Parametric Models of Dam and Levee Breaching*. PhD thesis, Clarkson University, Potsdam, NY, 30–56.

Wang, M., Feng, Y. T., Pande, G. N., Chan, A. H. C., and Zuo, W. X. (2017). Numerical modelling of fluid-induced soil erosion in granular filters using a coupled bonded particle lattice Boltzmann method. *Comput. Geotech.* 82, 134–143. doi: 10.1016/j.compgeo.2016.10.006

Wang, W., Chen, G., Zhang, H., Zhang, Y., and Zheng, L. (2017). Dynamic simulation of landslide dam behavior considering kinematic characteristics using a coupled DDA-SPH method. *Eng. Anal. Bound. Elem.* 80, 172–183. doi: 10.1016/j.enganabound.2017.02.016

Wang, W., Yang, J., and Wang, Y. (2020). Dynamic processes of 2018 Sedongpu landslide in Namcha Barwa–Gyala Peri massif revealed by broadband seismic records. *Landslides* 17, 409–418. doi: 10.1007/s10346-019-01315-3

Wang, Z., Cui, P., Yu, G., and Zhang, K. (2012). Stability of landslide dams and development of knickpoints. *Environ. Earth Sci.* 65, 1067–1080. doi: 10.1007/s12665-010-0863-1

Wang, Z., Melching, C. S., Duan, X., and Yu, G. (2009). Ecological and hydraulic studies of step-pool systems. *J. Hydraul. Eng.* 135, 705–717. doi: 10.1061/(asce)0733-9429(2009)135:9(705)

Wiegel, R. L. (1970). Water waves generated by landslides in reservoirs. *Proc. ASCE* 96, 307–333.

Wu, G. (2001). Earthquake-induced deformation analyses of the Upper San Fernando Dam under the 1971 San Fernando earthquake. *Can. Geotech. J.* 38, 1–15. doi: 10.1139/t00-086

Wu, W., and Li, H. (2017). A simplified physically-based model for coastal dike and barrier breaching by overtopping flow and waves. *Coast. Eng.* 130, 1–13. doi: 10.1016/j.coastaleng.2017.09.007

Wu, W., and Lin, Q. (2019). A 3-D finite volume model for sediment transport in coastal waters. *Ocean Dyn.* 69, 561–580. doi: 10.1007/s10236-019-01261-7

Xiong, X., Shi, Z. M., Guan, S. G., and Zhang, F. (2018). Failure mechanism of unsaturated landslide dam under seepage loading–Model tests and corresponding numerical simulations. *Soils Found.* 58, 1133–1152. doi: 10.1016/j.sandf.2018.05.012

Xu, F., Yang, X., and Zhou, J. (2017). Dam-break flood risk assessment and mitigation measures for the Hongshiyan landslide-dammed lake triggered by the 2014 Ludian earthquake. *Geomat. Nat. Hazards Risk* 8, 803–821. doi: 10.1080/19475705.2016.1269839

Xu, F. G., Yang, X. G., and Zhou, J. W. (2015). Experimental study of the impact factors of natural dam failure introduced by a landslide surge. *Environ. Earth Sci.* 74, 4075–4087. doi: 10.1007/s12665-015-4451-2

Yang, K. H., and Wang, J. Y. (2017). Experiment and statistical assessment on piping failures in soils with different gradations. *Mar. Geores. Geotechnol.* 35, 512–527. doi: 10.1080/1064119x.2016.1213338

Yang, X., Yang, Z., Cao, S., Gao, X., and Li, S. (2010). Key techniques for the emergency disposal of Quake lakes. *Nat. Hazards* 52, 43–56. doi: 10.1007/s11069-009-9350-y

Yin, Y., Wang, F., and Sun, P. (2009). Landslide hazards triggered by the 2008 Wenchuan earthquake, Sichuan, China. *Landslides* 6, 139–152. doi: 10.1007/s10346-009-0148-5

Zhang, F., and Ikariya, T. (2011). A new model for unsaturated soil using skeleton stress and degree of saturation as state variables. *Soils Found.* 51, 67–81. doi: 10.3208/sandf.51.67

Zhang, F., Li, M., Peng, M., Chen, C., and Zhang, L. (2019). Three-dimensional DEM modeling of the stress–strain behavior for the gap-graded soils subjected to internal erosion. *Acta Geotech.* 14, 487–503. doi: 10.1007/s11440-018-0655-4

Zhang, F., Wang, T., Liu, F., Peng, M., Furtney, J., and Zhang, L. (2020). Modelling of fluid-particle interaction by coupling the discrete element method with a dynamic fluid mesh: implications to suffusion in gap-graded soils. *Comput. Geotech.* 124:103617. doi: 10.1016/j.compgeo.2020.103617

Zhao, H. F., Zhang, L. M., and Xu, Y. (2013). Variability of geotechnical properties of a fresh landslide soil deposit. *Eng. Geol.* 166, 1–10. doi: 10.1016/j.enggeo.2013.08.006

Zhao, T. L., Chen, S. S., Fu, C. J., and Zhong, Q. M. (2018). Influence of diversion channel section type on landslide dam draining effect. *Environ. Earth Sci.* 77, 54–62.

Zhao, T. L., Chen, S. S., Fu, C. J., and Zhong, Q. M. (2019). Centrifugal model tests and numerical simulations for barrier dam break due to overtopping. *J Mt. Sci.* 16, 630–640. doi: 10.1007/s11629-018-5024-0

Zheng, H. C., Shi, Z. M., Peng, M., and Yu, S. B. (2018). Coupled CFD-DEM model for the direct numerical simulation of sediment bed erosion by viscous shear flow. *Eng. Geol.* 245, 309–321. doi: 10.1016/j.enggeo.2018.09.003

Zheng, X. G., Pu, J. H., Chen, R. D., Liu, X. N., and Shao, S. D. (2016). A novel explicit-implicit coupled solution method of SWE for long-term river meandering process induced by dambreak. *J. Appl. Fluid Mech.* 9, 2647–2660. doi: 10.29252/jafm.09.06.25969

Zhong, Q. M., Chen, S. S., Deng, Z., and Mei, S. A. (2019). Prediction of overtopping induced breach process of cohesive dams. *J. Geotech. Geoenviron. Eng.* 145:04019012. doi: 10.1061/(asce)gt.1943-5606.0002035

Zhong, Q. M., Chen, S. S., Mei, S. A., and Cao, W. (2018). Numerical simulation of landslide dam breaching due to overtopping. *Landslides* 15, 1183–1192. doi: 10.1007/s10346-017-0935-3

Zhou, G. G. D., Cui, P., Chen, H. Y., Zhu, X. H., Tang, J. B., and Sun, Q. C. (2013). Experimental study on cascading landslide dam failures by upstream flows. *Landslides* 10, 633–643. doi: 10.1007/s10346-012-0352-6

Zhou, G. G. D., Zhou, M., Shrestha, M. S., Song, D., Choi, C. E., Cui, K. F. E., et al. (2019). Experimental investigation on the longitudinal evolution of landslide dam breaching and outburst floods. *Geomorphology* 334, 29–43. doi: 10.1016/j.geomorph.2019.02.035

Zhou, M., Zhou, G. G. D., Cui, K. F. E., Song, D., and Lu, X. (2019). Influence of inflow discharge and bed erodibility on outburst flood of landslide dam. *J Mt. Sci.* 16, 778–792. doi: 10.1007/s11629-018-5312-8

Zhou, Y. Y., Shi, Z. M., Zhang, Q. Z., Jang, B. A., and Wu, C. Z. (2019). Damming process and characteristics of landslide-debris avalanches. *Soil Dyn. Earthq. Eng.* 121, 252–261. doi: 10.1016/j.soildyn.2019.03.014

Zhou, Z., Ranjith, P. G., and Li, S. (2016). Criteria for assessment of internal stability of granular soil. *Proc. Inst. Civil Eng. Geotech. Eng.* 170, 73–83. doi: 10.1680/jgeen.15.00165

Zhu, X. H., Peng, J. B., Jiang, C., and Guo, W. L. (2019). A Preliminary study of the failure modes and process of landslide dams due to upstream flow. *Water* 1: 1115. doi: 10.3390/w11061115

Zhu, Y. H., Visser, P. J., and Vrijling, J. K. (2004). "Review on embankment dam breach modeling," in *New Developments in Dam Engineering*, (London: Taylor & Francis Group), 1189–1196. doi: 10.1201/9780203020678.ch147

Zou, D., Xu, B., Kong, X., Liu, H., and Zhou, Y. (2013). Numerical simulation of the seismic response of the Zipingpu concrete face rockfill dam during the Wenchuan earthquake based on a generalized plasticity model. *Comput. Geotech.* 49, 111–122. doi: 10.1016/j.compgeo.2012.10.010

Conflict of Interest: The authors declare that the research was conducted in the absence of any commercial or financial relationships that could be construed as a potential conflict of interest.